Keratan sulfate affects sonic hedgehog signaling and regulates mouse spinal cord development

Hirokazu Hashimoto

DOCTOR OF PHILOSOPHY

Department of Physiological Sciences
School of Life Science
The Graduate University for Advanced Studies

2014

Acknowledgement

Foremost, I would like to express my sincere gratitude to my advisor Prof. Kazuhiro Ikenaka of National Institute for Physiological Sciences for providing me this opportunity to study in his laboratory. I appreciate his continuous support during my study and research, patience, motivation, enthusiasm, and immense knowledge, which guided me through research and writing this thesis.

Special thanks are expressed to Prof. Katsuhiko Ono, Dr. Hirohide Takebayashi, Dr. Seiji Hitoshi, Dr. Kenji Tanaka, Dr. Takeshi Shimizu, Dr. Takeshi Yoshimura and Dr. Yugo Ishino for providing me numerous ideas, valuable instructions, relevant discussions and help during my research work.

Beside my supervisors, I would like to thank the members of my thesis committee; Prof. Yumiko Yoshimura, Prof. Shinji Takada, and Prof. Kenji Kadomatsu for their encouragement, insightful comments, and hard questions.

I thank my fellow labmates in Prof. K. Ikenaka's lab: Dr. Naoko Inamura, Dr. Shota Sugio, Wilaiwan Wisessmith, Yasuyuki Osanai, Jiang Wen, Mai Narumi, Kazuo Kunisawa, Li Jia Yi and Saori Kikuchihara for the stimulating discussions and for all the fun we had in the last three years.

Table of Contents

Abbreviations

AMN: Autonomic motor neuron

BMP: Bone morphogenetic protein

CNS: Central nervous system

DAB: Diaminobenzidine

FP: Floor plate

GAG: Glycosaminoglycan

GlcNAc: N-acetylglucosamine

HS: Heparan sulfate

HRP: Horseradish peroxidase

KS: Keratan sulfate

MBP: Myelin basic protein

MN: Motor neuron

Ngn2: Neurogenin 2

OPC: Oligodendrocyte precursor cell

PDGFRα: Platelet-derived growth factor receptor alpha

RP: Roof plate

RT-PCR: Reverse transcription polymerase chain reaction

Shh: Sonic hegdehog

SMN: Somatic motor neuron

SDS: Sodium dodecylsulfate

VZ: Ventricular zone

Summary

Neurons and glial cells of the central nervous system (CNS) are generated from neural stem cells in a highly specific manner, both spatially and temporally. In the embryonic spinal cord, several secretory factors, such as Wnt, BMP and Shh, act as morphogen and regulate development. Wnt and BMP are secreted from the roof plate, and Shh are secreted from the floor plate and the notochord. They are involved in the patterning of the spinal cord. Wnts and Shh bind to acidic sugar chains, for example, heparan sulfate, chondroitin sulfate and keratan sulfate. I hypothesized that the interaction between morphogens and acidic sugar chains play essential roles in the pattern formation of embryonic spinal cord. In this study, I analyzed involvement of keratan sulfate.

Keratan sulfate is a glycosaminoglycan. It is composed of repeating disaccharide units of galactose and N-acetylglucosamine (GlcNAc), where the C6 position of GlcNAc is always sulfated. Keratan sulfate is expressed in the cornea, cartilage, bone and the CNS during development. Although there are several reports showing that keratan sulfate is an important factor for the glial scar formation following an injury, corneal development and healing, function of keratan sulfate in the spinal cord development remains to be investigated.

First, I analyzed localization of keratan sulfate in the embryonic spinal cord. Highly sulfated keratan sulfate was expressed in the floor plate and the notochord. This

expression pattern colocalized with Shh expression. Genes of all the enzymes involved in keratan sulfate synthesis were expressed in the embryonic mouse spinal cord. Next, to understand roles of keratan sulfate, I analyzed the keratan sulfate null mouse spinal cord. This mouse is deficient for GlcNAc6ST-1, which is essential for keratan sulfate chain elongation. I first examined the position of domain structures by in situ hybridization and immunohistochemistry. I could not find any change at E10.5. At E12.5, however, the domain structure shifted ventrally in the keratan sulfate null spinal cord; pMN domain shifted ventrally and the length of p2 and p3 domain was decreased. Formation of these domain structures are controlled by Shh signaling. Thus I checked the Shh signaling as well as Wnt signaling, representing dorsal morphogens. Wnt signaling was monitored by the expression of Axin2, which did not change between wild type (WT) and keratan sulfate null mice at E10.5 and E12.5. Expression of Shh signaling reporter gene, Patched1, also did not change between WT and keratan sulfate null mice at E10.5. However, at E12.5, Patched1 expression pattern was different between WT and keratan sulfate null mice. I thus focused on Sulf1, heparan sulfate endosulfatase, involved in the Shh signaling and oligodendrocyte development. In the E12.5 keratan sulfate null mice, the length of Sulf1 expressing region was decreased. It is possible that keratan sulfate regulates Sulf1 expression in the embryonic spinal cord via alternation of Shh signaling since Sulf1 expression is regulated by Shh signaling.

These phenotypes may affect differentiation of neural stem cells in the embryonic spinal cord. I focused on cell types generated from the pMN domain. The pMN domain generates motor neurons and subsequently oligodendrocytes. PDGFRα, a marker for

oligodendrocyte precursor cell, was hardly detected in the E12.5 spinal cord. In addition, at E14.5 the number of oligodendrocyte precursor cells still tended to be decreased. Moreover, motor neuron production analyzed by Islet1/2 immunohistochemistry was increased at E12.5. These excessively generated motor neurons were eliminated by apoptosis and microglial phagocytosis at later stages. On the other hand, decrease in the number of oligodendrocyte lineage cells was caught up by P0.

Finally, since pMN domain position shifted ventrally in keratan sulfate null mice, I investigated oligodendroglial specification whether the switch from motor neuron production to oligodendrocyte production was abnormal in the pMN domain. Oligodendroglial specification is marked by the induction of the SOX10 expression. Following that, coexpression of Olig2 with Nkx2.2 promotes oligodendrocyte differentiation. I observed the SOX10 expression at E12.5, which did not change between wild type and keratan sulfate null mice. As another oligodendroglial specification marker, I analyzed the number of Olig2, Nkx2.2 double positive cells in the pMN domain. The number of double positive cells was decreased in keratan sulfate null mice. On the other hand, I investigated motor neuron specification. Motor neuron is specified by coexpression of Olig2 and Ngn2 in the pMN domain. Olig2, Ngn2 double positive cells number was significant increased in the pMN domain. This result indicated that motor neuron generation was continued. Thus switching of motor neuron generation to oligodendrocyte generation was abnormal in the pMN domain.

Taken together, my study suggests that keratan sulfate chain plays important role in the pattern formation and oligodendrocyte development in the embryonic spinal cord.

Introduction

Neurons and glial cells of the central nervous system are generated from neural stem cells in a highly specific manner, both spatially and temporally. The spinal cord has served as an excellent model for studying both diversity and successive waves of neural cell generation. In the embryonic spinal cord, several secretory factors, such as Wnt, BMP and Shh, act as morphogen and regulate development. Wnt and BMP are secreted from the roof plate and Shh are secreted from the floor plate and the notochord. They are involved in the pattern formation and the development of the spinal cord. Wnt-1, -3, -3a and -4 have been reported to be expressed in the dorsal region of embryoni spinal cord and regulate oligodendrocyte development **(Shimizu et al., 2005)**. Morphogens are long-range signaling molecules that pattern developing spinal cord in a concentration-dependent manner. Morphogens gradient was classically thought to be formed by free diffusion. However, imaging of morphogen distribution indicated that their localization could not be explained by simple diffusion. It was more likely that morphogens localizes on specific structures of cell membrane, such as glycan or lipid raft. Wnts and Shh has a Cardin-Weintraub motif (XBBBXXBX, where B is a basic residue and X is any residue) and bind to acidic sugar chains **(Farshi et al., 2011, Chang et al., 2011, Nadanaka et al., 2008)**.

Acidic sugar chains have two types of glycan, sialylated oligosaccharides and sulfated oligosaccharides. Especially, sulfated oligosaccharides are represented by glycosaminoglycans, such as heparan sulfate, chondroitin sulfate, dermatan sulfate and

keratan sulfate. These oligosaccharides are attached as a side chain to proteoglycans found on the cell surface and in the extracellular matrix, and it modulates signals that initiate differentiation during development. Last year, Touahri et al. reported that heparan sulfate endosulfatase, Sulf1, regulated Shh signaling and oligodendrocyte differentiation in the embryonic spinal cord **(Touahri et al., 2012)**. In addition, Wnt3a binds to specific structure containing E-disaccharide units of chondroitin sulfate (CS-E) with high affinity **(Nadanaka et al., 2008)**. This CS-E structure enhances Wnt3a signaling **(Nadanaka et al., 2008, Nadanaka et al., 2011)**. Although heparan sulfate and chondroitin sulfate in the embryonic spinal cord was extensively studied, the function of keratan sulfate is less known in the developing spinal cord.

Keratan sulfate is sulfated glycosaminoglycan. It is composed of repeating disaccharide units of galactose and N-acetylglucosamine, where the C6 position of GlcNAc is always sulfated. Keratan sulfate is expressed in the cornea, cartilage, bone and the central nervous system during development. There are several reports showing that keratan sulfate is an important factor for the glial scar formation following an injury **(Zhang et al., 2006, Ito et al., 2010, Hilton et al., 2012 Kadomatsu and Sakamoto, 2013)** and is enhanced in microglia/macrophages and the extracellular matrix after spinal cord injuly **(Jander et al., 2000, Jones et al., 2002)**. In addition, other group reported that corneal keratan sulfate bound with high affinity to FGF-2 and Shh involved in corneal development and healing **(Weyers et al., 2013)**.

In regard to development of embryonic spinal cord, the formation of several domain structures depends on the expression of transcription factors **(Helm and**

Johnson et al., 2003, Tanabe and Jessell et al., 1996). These transcription factors are regulated by morphogens. Shh regulates ventral transcription factors, and Wnt and BMP regulate the dorsal transcription factors. Especially, Shh forms a concentration gradient along the ventral-dorsal axis of the neural tube and functions as a morphogen to induce the expression of Class II transcription factors, such as Olig2, Nkx2.2and Nkx6.1, and at the same time represses the expression of Class I transcription factors, such as Pax6, Irx3 and Dbx2 **(Zhou and Anderson, 2002, Jacob and Briscoe, 2003, Briscoe et al., 2008) (see Figure1)**. It is known that a certain subtype of neurons, such as motor neurons and interneurons, are generated from a particular domain structure. Glial cells, such as oligodendrocytes, also develop from a particular domain structure (pMN domain) of the ventral spinal cord. The Olig2 gene is expressed in the pMN domain and is essential for their generation. Though motor neurons and oligodendrocytes share the same progenitor domain in the ventral spinal cord, they are generated at different time points, with neurogenesis preceding gliogenesis **(Sugimori et al., 2007, Guillemot et al., 2007)**. Transient neurogenin1 and neurogenin2 expression in the pMN domain promotes neurogenesis, but when their expression is downregulated, gliogenesis is initiated **(Zhou and Anderson et al., 2002)**. In addition, oligodendroglial specification is marked by the induction of Sox10 expression in the pMN domain. This Sox10 expression is upregulated by Olig2 **(Küspert et al., 2011)**. Following that, coexpression of Olig2 with Nkx2.2 in the spinal cord promotes oligodendrocyte differentiation **(Zhou et al., 2001)**. Since these neural developments is controlled by the Shh signaling, it is possible that acidic sugar chain regulates morphogen (including Shh) signaling and/or

distribution in the embryonic spinal cord.

In this study, I hypothesized that the interaction between morphogens and acidic sugar chains play essential roles in the pattern formation of embryonic spinal cord and investigated the role of keratan sulfate played in the development of the embryonic spinal cord.

Materials and Methods

Antibodies

Primary antibodies used in this study were as follows; mouse anti-keratan sulfate IgG (5D4, Cosmo Bio Co.), mouse anti-Shh IgG (5E1, Developmental Studies Hybridoma Bank), mouse anti-Nkx2.2 IgG (74.5A5,DSHB), mouse anti-Pax7 IgG (DSHB), rabbit anti-Pax6 IgG (Chemicon), rabbit anti-Olig2 IgG (Chemicon), mouse anti-Nkx6.1 IgG (DSHB), rat anti-MBP IgG (Millipore), mouse anti-Islet1/2 IgG(DSHB), rabbit anti-Cleaved Caspase-3 IgG (Cell Signaling Technology), rabbit anti-Iba1 IgG(Wako)

For immunocyto/histochemistry, I used Alexa 488-conjugated anti-rabbit IgG (Invitrogen), Alexa 568-conjugated anti-rabbit IgG (Invitrogen), Alexa 488-conjugated anti-mouse IgG (Invitrogen) and Alexa 568-conjugated anti-mouse IgG (Invitrogen) as secondary antibodies.

Animals

All mice used in this experiment were kept in the institutional Center for Experimental Animals with free access to food and water. Timed pregnant B6J (C57BL/6J) mice were purchased from Charles River (Yokohama, Japan), or mice were

mated to obtain pregnant mice. Noon of the plugged date was considered as embryonic day (E) 0.5. All experiments were carried out under the permission of the institutional Animal Research Committee.

RT-PCR

Total RNA was isolated using Sepazol (Nacalai tesque) and RNA concentration was quantified by a spectrophotometer at 260 nm (NanoDrop Technologies, DE, USA). One μg of total RNA was used to synthesize cDNA with olig-d$(T)_{12\text{-}18}$ primers (GE Healthcare) and MoMLV reverse transcriptase (ReverTra Ace; TOYOBO) in a 20 μl reaction mixture at 42°C for 1 hour. The PCR reaction mixture (20 μl) consisted of 0.5 μl of cDNA, 16 pmol each of 5′ and 3′ primers, 0.2 mM dNTP, 1.5 mM Mg^{2+}, 2 μl of PCR reaction buffer, and 0.8 units of Taq polymerase (Promega). cDNA was amplified in a thermal cycler (Perkin-Elmer) with denaturation at 95°C for 30 seconds, annealing at 55°C for 30 seconds and extension at 72°C for 30 seconds for 30 cycles. Primer sequence is shown in Table1.

Tissue preparation

Keratan sulfate null (GlcNAc6ST-1 deficient) mice were provided by Dr. Kenji Kadomatsu in Nagoya University. Wild type B6J (C57BL/6J) pregnant mice at postcoitum day 10.5, 11.5, 12.5, 14.5 and postnatal day 0 were deeply anesthetized by

intraperitoneal injection of 50 mg/kg of pentobarbital, and their offspring were removed from the uterus. The pups were perfusion-fixed with 4% paraformaldehyde (PFA) in PBS through the heart, and then brains were removed and post-fixed with 4% PFA/PBS overnight at 4°C. The pups were cryoprotected with 20% sucrose/PBS, embedded in Tissue-Teck Optimal Cutting Temperature (OCT) compound (Sakura Finetechnical Co. Ltd., Tokyo, Japan), and quickly frozen in liquid nitrogen. Spinal cords were sectioned at 20-μm thickness by a cryostat (CM-3050; Leica, Bensheim, Germany) and thaw mounted onto RNase-free methyl-amino-serum (MAS)-coated glass slides (Matsunami Glass, Japan). These sections were used for in situ hybridization and immunohistochemistry.

In Situ Hybridization

Digoxigenin (DIG)-labeled single strand riboprobes was synthesized using T7, T3 or SP6 RNA polymerase and DIG RNA labeling mix (Roche). In situ hybridization was performed as described previously (Ding et al., 2005). Briefly, the sections were treated with proteinase K (1 μg/ml for 30 minutes at room temperature) and hybridized overnight at 60°C with DIG-labeled antisense or sense riboprobes in a hybridization solution consisting of 40% formamide, 20 mM Tris-HCl (pH 7.5), 600 mM NaCl, 1 mM EDTA, 10% dextran sulfate, 200 μg/ml yeast tRNA, 1 X Denhardt's solution and 0.25% SDS. Sections were washed three times in 1 x SSC (150 mM NaCl and 15 mM trisodium citrate) containing 50% formamide at 60°C, followed by 0.1 M maleic buffer

(pH 7.5) containing 0.1% Tween 20 and 0.15 M NaCl. The bound DIG-labeled probe was detected by overnight incubation of the sections with anti-DIG antibody conjugated to alkaline phosphatase (1:2000; Roche) and color developed in the presence of 4-nitroblue tetrazolium chloride, 5-bromo-4-chloro-3-indolylphosphate and levamisol in dark at room temperature. After alkaline phosphatase-mediated visualization, some sections were incubated with anti-Olig2 antibody, followed by Biotin-conjugated secondary antibody and visualized using an ABC Elite kit (Vector Laboratories, Burlingame, CA) and diaminobenzidine as a chromogen. Sections were washed in cold PBS to quench the reaction and mounted with Permount (Fischer Scientific, PA, USA) after serial dehydration.

Immunohistochemistry

Transverse cryosections at 20-μm thickness of the embryonic spinal cord were immunostained as follows. In spinal cord sections stained with antibodies against Nkx2.2, Pax7, Pax6, Olig2, Nkx6.1, MBP, Islet1/2, Cleaved Caspase-3 or Iba1, citrate antigen retrieval was performed. Sections were treated with heat in a microwave oven (550W) for 5 min in 10 mM citrate buffer (pH 6.0) and cooled down to room temperature. After antigen retrieval, the sections were blocked with 10% normal goat serum/PBS containing 0.1% Triton X-100 for 1 hour and then incubated with primary antibodies in the blocking buffer at 4°C overnight. After washing with PBS-T (0.1% Triton X-100/PBS), they were incubated with Alexa 488- and/or Alexa568-conjugated

secondary antibodies (Invitrogen Molecular Probes, USA) diluted in the blocking buffer for two hours at room temperature, followed by washes in PBS. The nuclei of cells were counterstained with Hoechst 33342 (0.1 μg/ml; Sigma, USA). For diaminobenzidine (DAB) visualization, sections were treated with 0.3% Triton X-100 in PBS for 5 min at room temperature, followed by the treatment with 3% H_2O_2 to block endogenous peroxidase activity for 30 min at room temperature. After incubation in the blocking buffer, sections were incubated overnight with primary antibodies at 4℃, followed by the treatment with secondary antibodies conjugated with biotin for 60 min at room temperature. After washing with PBS, sections were then incubated with avidin-biotin-peroxidase complex (Vectastain Elite ABC kit, Vector Laboratories, CA, USA) for 60 min at room temperature. Immune complex was visualized by immersion of sections in 0.05% DAB/0.015% H_2O_2.

Keratan sulfate and Shh Immunohistochemistry

The pups were embedded in OCT compound and quickly frozen in liquid nitrogen. Spinal cords were sectioned at 20-μm thickness by a cryostat and thaw mounted onto MAS-coated glass slides. These sections were fixed with cold acetone (-30℃) for 15 minutes. After fixation, the sections were blocked in 3% bovine serum albumin (Sigma, USA) in PBS for 1 hour and then incubated with primary antibodies in the blocking buffer at 4°C overnight. After washing with PBS, they were incubated with Alexa 488-conjugated secondary antibodies diluted in the blocking buffer for two hours

at room temperature, followed by washes in PBS-T (0.1% Triton X-100/PBS). The nuclei of cells were counterstained with Hoechst 33342.

Statistics

Statistical analysis was performed using an unpaired two-tailed Student's t-test if applicable. Level of significance was set at $p < 0.05$.

Results

Expression of keratan sulfate in the embryonic spinal cord

To understand the function of keratan sulfate in the central nervous system, it is important to know where keratan sulfate is expressed in the embryonic spinal cord. I assessed the localization of keratan sulfate in the embryonic spinal cord by immunohistochemistry using cross cryosections of spinal cords from mouse embryos at E10.5. I used 5D4 antibody, recognizing highly sulfated keratan sulfate structure. At E10.5, keratan sulfate was expressed in the floor plate and the notochord **(Figure2B, E)**. At the same time, I stained the spinal cord with Shh (5E1) and Nkx2.2, a marker for p3 domain, by immunohistochemistry and compared. Highly sulfated keratan sulfate colocalized with Shh at the floor plate **(Figure2A, D)**. However, keratan sulfate was not expressed in the p3 domain **(Figure2C, F)**. Next, I analyzed expression of keratan sulfate synthase by RT-PCR and *in situ* hybridization. In RT-PCR, all the keratan sulfate synthases were found to be in all stages examined **(Figure3)**. Especially, GlcNAc6ST-1, a key enzyme for keratan sulfate chain elongation, was strongly expressed during these stages. Since keratan sulfate was expressed in the floor plate and the notochord, it is possible that keratan sulfate affects Shh signaling and regulates the mouse embryonic spinal cord development.

The domain structure shifted ventrally in the keratan sulfate null mice at E12.5, but not at E10.5

To analyze the function of keratan sulfate in the embryonic spinal cord, I investigated keratan sulfate null mice **(Uchimura et al., 2004)**. This mouse did not express GlcNAc6ST-1 gene and could not elongate the keratan sulfate chains. I first examined the position of domain structures by in situ hybridization and immunohistochemistry. As domain markers, I used Math1, Olig3, Pax7, Nkx6.1, Olig2 and Nkx2.2 RNA probes **(Figure1)**. At E10.5, domain structures did not change in the keratan sulfate null mice **(Figure4A-L)**. On the other hand, domain structures at E12.5 seemed to shift ventrally in keratan sulfate null mice **(Figure5G-L)**. Thus, I confirmed this observation by immunohistochemistry using Pax7, Pax6, Nkx6.1, Olig2 and Nkx2.2 antibodies **(Figure6A-F)**, and got similar results in accordance with *in situ* hybridization at E12.5. The pMN domain, the Olig2 positive region, shifted ventrally and the length of p2 domain and p3 domain, the Nkx2.2 positive region, decreased at E12.5 **(Figure6G)**. In addition, the length of dorsal domain structures, Olig3 and Pax7 positive regions, was increased. Domain structures shifted ventrally in keratan sulfate null mice, suggesting keratan sulfate affects Shh signaling.

Alternation of morphogens signaling at E12.5

Morphogens play important role in pattern formation of the embryonic spinal

cord. In addition, keratan sulfate was expressed in the floor plate. To assess the effect of morphogen signaling in the keratan sulfate null mice, I performed in situ hybridization, using Axin2 and Patched1 RNA probes. Axin2 is a canonical Wnt signaling reporter and Patched1 is a Shh signaling reporter. In WT mice at E10.5, Axin2 was expressed around the roof plate and in the ventral region; the border between mature motor neuron layer and the pMN domain **(Figure7A)**. At E12.5, Axin2 was only expressed in the roof plate and the ventral expression disappeared in WT mice **(Figure7C)**. In E10.5 and E12.5 keratan sulfate null mice, Axin2 expression pattern did not change **(Figure6B, D)**. So canonical Wnt signaling was not affected in keratan sulfate null mice. However, the contribution of non-canonical Wnt signaling in keratan sulfate null mice remains to be elucidated. Patched1 was broadly expressed in the ventral region, except for the floor plate and mature motor neuron layer in E10.5 WT mice **(Figure8A)**. At E11.5, Patched1 expression was observed in the ventral VZ, except for the floor plate. Especially, its expression was concentrated in the pMN domain of WT mice **(Figure8C)**. At E12.5 Patched1 was expressed in the VZ, except for the floor plate. At this age, Patched1 mRNA accumulation in the pMN domain disappeared **(Figure8E)**. In the E10.5 and E11.5 keratan sulfate null mice, Patched1 expression pattern did not change **(Figure8B, D)**. However, in the keratan sulfate null mice at E12.5, Patched1 mRNA was accumulated in the ventral region **(Figure8F)**. Then I investigated the domain in which Patched1 mRNA was accumulated by staining with a domain marker, Olig2 antibody. Accumulated Patched1 mRNA colocalized with Olig2 **(Figure8F)**. In contrast, in the p3domain and floor plate, Patched1 expression was weak. The pattern of

Shh signaling differed between WT and keratan sulfate null spinal cords. This finding also indicates that keratan sulfate regulates Shh signaling.

Dorsal expansion of Sulf1 domain was decreased in the keratan sulfate null mice at E12.5

Previously, Shh signaling was shown to be regulated by heparan sulfate chain **(Chang et al., 2011)**. Especially, heparan sulfate endosulfatase (Sulf1) was reported to regulate Shh signaling activity and to be involved in the oligodendroglial fate decision **(Danesin et al., 2006, Touahri et al., 2012)**. Thus 6-sulfo-heparan sulfate pattern plays an important role in their interactions with Shh. Dr. Yugo Ishino and Jiang Wen, my group mates in Ikenaka lab, studied the developmental effect of Sulf1/2 in the embryonic spinal cord. They revealed that Sulf1 was initially expressed in the floor plate at E10.5 and, thereafter, Sulf1 expression expanded dorsally at E11.5 and E12.5 **(Figure9C, E)**. In addition, deleting of Sulf1 and/or Sulf2 genes affected the Shh signaling pattern and regulated oligodendrocyte development (manuscript in preparation). On the other hand, Weyers et al. reported that keratan sulfate binds to FGF-2 and Shh **(Weyers et al., 2013)**. So keratan sulfate and heparan sulfate may collaborate to regulate the development of the embryonic spinal cord. Therefore, I analyzed the Sulf1 expression from E10.5 to E12.5 in the keratan sulfate null spinal cord **(Figure9A-F)**. In the E12.5 keratan sulfate null mice, Sulf1 expression pattern was different from that of WT **(Figure9E, F and Figure10A)**. In addition the dorsal

expansion of Sulf1 expression was decreased to about 20% of WT in the keratan sulfate null mice **(Figure10B)**. The weak Sulf1 expansion may have affected the Shh signaling in keratan sulfate null mice.

The number of oligodendrocyte precursor cells was hardly expressed in the E12.5 keratan sulfate null mice

Since domain structures and pattern of Shh signaling differed between wild type (WT) and keratan sulfate null mice at E12.5, it is possible that keratan sulfate affects cell fate, such as neuron, oligodendrocyte and astrocyte, in the embryonic spinal cord. In Sulf1 deficient mice, oligodendrocyte generation was impaired at E12.5 **(Touahri et al., 2012)**. I focused on the development of pMN domain. In the early stage (E9.5-11.5), motor neuron (MN) is generated from the pMN domain and after that oligodendrocyte precursor cells (OPCs) generation begins (E12.5-). To analyze the development of the oligodendrocyte at E12.5 and E14.5, I performed in situ hybridization, using PDGFRα, a marker for oligodendrocyte precursor cells. In keratan sulfate null mice, the number of PDGFRα positive cells was significantly decreased at E12.5 **(Figure11A-C)**. Also, at E14.5, number of OPCs was decreased **(Figure11D-F)**. Especially, OPCs in the dorsal region was markedly reduced.

Oligodendrocyte generation caught up by postnatal 0 in keratan sulfate null mice

Since oligodendrocyte precursor cells generation was decreased in embryonic stages, I examined whether oligodendrocyte development would be caught up at later stages. I stained the spinal cord with antibodies against myelin basic protein (MBP), a marker for oligodendrocyte, and Olig2 at postnatal day 0 (P0). In keratan sulfate null mice, the number of oligodendrocytes was no more decreased at P0 **(Figure12A-D)**. These results clearly demonstrate that keratan sulfate plays a role in the control of ventral OPC generation.

Motor neuron generation continued to E12.5 in keratan sulfate null mice

Since OPCs generation was delayed at E12.5, it is possible that MN generation was still continued at E12.5. To assess the MN generation, I stained embryonic spinal cords with Islet1/2 antibody, as a MN marker. There are two types of mature MN, autonomic motor neurons (AMNs) and somatic motor neurons (SMNs) in the ventral horn of spinal cord **(Wetts and Vaughn, 2000)**. In addition, there are immature MNs migrating from the pMN domain. I analyzed the number of Islet1/2 positive cells in the ventral horn. Both the numbers of AMNs and SMNs were significantly increased in the E12.5 keratan sulfate null mice **(Figure13A-C)**. Number of immature MNs assessed by counting Islet1/2 positive cell number emerging from the pMN domain (shown in the dotted square in Figure13D, E) was also increased in the medial region **(Figure13D-F)**. These results suggest that MN generation was still continued in keratan sulfate null mice at E12.5.

Excessively generated motor neurons was eliminated by apoptosis and microglial phagocytosis

Since MNs were generated excessively at E12.5, I asked whether the number of motor neuron was adjusted by E14.5. Thus I investigated the induction of apoptosis using anti-cleaved caspase-3 antibody and microglia activation using anti-Iba1 antibody. In the ventral horn of spinal cord, the induction of apoptosis was significantly increased **(Figure14A-C)** and microglia was activated in keratan sulfate null mice **(Figure14D, E)**. Therefore the excessively generated MNs were eliminated in keratan sulfate null mice.

Switching of motor neuron to oligodendocyte generation was delayed in the keratan sulfate null mice

Lastly, I analyzed oligodendroglial specification whether the switching of motor neuron generation to oligodendrocyte generation is delayed in keratan sulfate null mice. Oligodendroglial specification is marked by the induction of the SOX10 expression **(Kuhlbrodt et al., 1998, Zhou et al., 2000, Stolt et al., 2002)**. SOX10 is specifically upregulated in Olig2 progenitors fated to generate OPCs as early as E11.5, and its expression is further maintained during OPC migration in the ventricular zone **(Zhou et al., 2000)**. Following that, coexpression of Olig2 with Nkx2.2 promotes

oligodendrocyte differentiation **(Figure15A)**. NKx2.2 is initially expressed in the p3 domain, which generates V3 interneurons **(Briscoe et al., 1999, Liu et al., 2002)**. After that, at later stages, Nkx2.2 expression is specifically upregulated in Olig2 positive OPCs either immediately before they migrate out of VZ in chicken **(Xu et al., 2000, Soula et al., 2001, Zhou et al., 2001, Fu et al., 2002)** or after they disperse into the white matter region in rodents **(Fu et al., 2002)**. Thus I stained the spinal cord with Sox10 RNA probe or Olig2 and Nkx2.2 antibodies. Sox10 was expressed in keratan sulfate null mice, similar to the WT, at E12.5 **(Figure15B, C)**. In contrast, the number of Olig2 and Nkx2.2 double positive cells was significantly decreased **(Figure15D-F)**. Therefore the switching of MN generation to oligodendrocyte generation was abnormal at E12.5.

I also investigated motor neuron specification. The basic helix-loop-helix (bHLH)-class transcription factors Ngn1/2 and Olig1/2 play important roles on motor neuron generation **(Scardigli et al., 2001, Lu et al., 2002, Zhou and Anderson 2002)**. Coexpression of Olig2 and Ngn2 in pMN domain occurs during the period of motor neuron generation, however, at later stages when oligodendrocytes were produced, Ngn2 expression becomes downregulated **(Sun et al., 2001, Zhou et al., 2001; Figure16A)**. To analyze the motor neuron specification, I stained the spinal cord with Olig2 antibody and Ngn2 RNA probe. Ngn2 expression was observed in the pMN domain and colocalized with Olig2 positive cells in keratan sulfate null mice at E12.5 **(Figure16B-F)**. This result supports that MN generation is continued at E12.5 and is consistent with elevation of Islet1/2 positive cells.

Taken together, in keratan sulfate null mice, switching of motor neuron to oligodendrocyte generation was abnormal at E12.5. As a result, oligodendrocyte differentiation was delayed and motor neuron generation continued.

Discussion

In the present study, I focused on the relationship between Shh signaling and acidic sugar chain, such as keratan sulfate, heparan sulfate and showed that keratan sulfate affects Shh signaling and regulates the switching of motor neuron to oligodendrocyte generation.

The secreted factor Shh acts as morphogen and organizes the pattern of cellular differentiation in the ventral neural tube. In chick and mouse embryos, floor plate (FP) specification involves a biphasic response to Shh signaling that controls the dynamic expression of key transcription factors, such as FoxA2, Arx. FP induction depends on high level of Shh signaling. Subsequently, however, prospective FP cells become refractory to Shh signaling **(Ribes et al., 2010)**.

Keratan sulfate was originally identified as the major glycosaminoglycan (GAG) of cornea but is now known to modify several proteins in a wide variety of tissues **(Funderburgh, 2002)**. In the central nervous system (CNS), when keratan sulfate is induced after spinal cord and brain injury, induced keratan sulfate inhibit the axonal regeneration and sprouting **(Imagama et al., 2011)**. Weyer et al. reported that in the bovine corneal, keratan sulfate binds with high affinity to FGF-2 and Shh, and involves in the corneal development and healing **(Weyer et al., 2013)**. In my research, I observed that highly sulfated keratan sulfate localized in the floor plate and the

notochord **(Figure2B, E)**. I think that this expression involves in Shh distribution and/or signaling. To estimate roles of keratan sulfate, I performed experiments using keratan sulfate null mice. I revealed that keratan sulfate affects the Shh signaling pattern, and regulates development of the embryonic spinal cord through ventral shifts of domain structures that express Olig2 and Nkx2.2.

Heparan sulfate play crucial roles in numerous signaling and Sulf1, by remodeling heparin sulfate 6-O-sulfation pattern, is recognaized as a key regulator of the interactions with signaling molecules, such as Shh **(Danesin et al., 2006, Ratzka et al., 2008, Wojcinski et al., 2011, Touahri et al., 2012)**. Sulf1 is well known to remove 6-O-sulfate groups on heparan sulfate chains of heparan sulfate proteoglycan (HSPG) **(Lamanna et al., 2007)**. Therefore, loss of Sulf1 in mice increases the amount of trisulfated disaccharides and proportionately decreses disulfated ones **(Ai et al., 2006, Lamanna et al., 2006, Nagamine et al., 2012)**. Importantly, Shh is known to preferentially bind to heparan sulfate chains having a high level of sulfation **(Carrasco et al., 2005, Zhang et al., 2007, Dierker et al., 2009)** and Sulf1 activity is likely to lower interaction between Shh and heparan sulfate. On the other hand, Touahri et al. indicated that Sulf1 is dispensable for the formation of the shh-dependent ventral progenitors domains that express Olig2 and Nkx2.2, and regulates the oligodendrocyte development **(Touahri et al., 2012)**. In addition, my group gets the same result in Sulf1 and/or Sulf2 null mice. Sulfs affects Shh signaling, but it is unnecessary for the formation of ventral domain structures. The loss of Sulfs regulates the oligodendrocyte

development.

Here, I describe my hypothesis for the regulation of domain shift in the keratan sulfate null mice **(Figure17)**. In WT mice, since Sulf1 is expressed in the floor plate at E10.5 **(Figure9A)**, it is likely to decrease the 6O-sulfated heparan sulfate structures in the floor plate. After that, weak Sulf1 signal expanded dorsally from the floor plate at E11.5 and E12.5 **(Figure9C, E)**. In these stages, 6O-sulfated heparan sulfate structures should be also decreased in Sulf1 expanded regions, such as p3 and the pMN domains. As a result, it is difficult for heparan sulfate to bind to Shh any more in Sulf1 expressed area and upregulate Shh signaling just dorsal to the Sulf1 expressed area. Highly sulfated keratan sulfate initially binds to Shh in the floor plate. After that, Shh is transferred from keratan sulfate to 6O-sulfated heparan sulfate, thereby out of exiting the floor plate. When Shh signaling accumulates in the pMN domain at E11.5, oligodendrocyte development begins from E12.5. In keratan sulfate null mice, Shh cannot bind to keratan sulfate and heparan sulfate in the floor plate. So Shh is not transported dorsally. Consequently, it is possible that Shh signaling activity is decreased and the ventral domain is shifted ventrally at E12.5.

Through these studies, I found that Axin2 was expressed in the ventral region; in the border between motor neuron layer and the pMN domain. This result indicated that canonical Wnt protein is present in this region. In the embryonic spinal cord, Wnt-1, -3, -3a, canonical Wnts, mainly acts on the oligodendrocyte development **(Shimizu et al.,**

2005). In addition, Wnt3 released by spinal lateral motor neuron regulates the arborization and presynaptic differentiation of neurotrophin 3 sensory neurons but not nerve growth factor (NGF)-responsive sensory neurons **(Krylova et al., 2002, Ciani and Salinas, 2005)**. So it is possible that Wnt3 is candidate for canonical Wnt pathway in the ventral region. To analyze which Wnts is expressed in the ventral region at each stage, from E10.5 to E12.5, I performed in situ hybridization using several Wnts RNA probes, including canonical and non-canonical Wnts. However, I could not detect the canonical Wnt gene in the ventral region. On the other hand, I found some non-canonical Wnt gene in the ventral region, such as Wnt-4, Wnt-7a, Wnt-7b and Wnt11 (data not shown). These non-canonical Wnt gene function is not well known in the embryonic spinal cord.

In conclusion, my data indicates that keratan sulfate plays important roles in the formation of ventral domain structures and Shh signaling. As a result, keratan sulfate regulates the oligodendrocyte development. Since most of studies on keratan sulfate analyzed the effect at the postnatal and adult stages **(Hirano et al., 2013)**, my study is the first report describing the function of keratan sulfate in the embryonic spinal cord.

Reference

Briscoe J, Sussel L, Serup P, Hartigan-O'Connor D, Jessell TM, Rubenstein JL, Ericson J (1999). Homeobox gene Nkx2.2 and specification of neuronal identity by graded Sonic hedgehog signalling. Nature, 398, 622-627

Briscoe J, Novitch BG(2008). Regulatory pathways linking progenitor patterning, cell fates and neurogenesis in the ventral neural tube. Philosophical Transactions of the Royal Society B-Biological Sciences, 363, 57-70

Chang SC, Mulloy B, Magee AI, Couchman JR (2011). Two distinct sites in sonic Hedgehog combine for heparan sulfate interactions and cell signaling functions. Journal of Biological Chemistry, 286, 44391-44402

Ciani L, Salinas PC (2005). WNTs in the vertebrate nervous system: from patterning to neuronal connectivity. Nature Reviews Neuroscience, 6, 351-362

Danesin C, Agius E, Escalas N, Ai X, Emerson C, Cochard P, Soula C (2006). Ventral neural progenitors switch toward an oligodendroglial fate in response to increased Sonic hedgehog (Shh) activity: involvement of Sulfatase 1 in modulating Shh signaling in the ventral spinal cord. Journal of Neuroscience, 6, 5037-5048

Farshi P, Ohlig S, Pickhinke U, Höing S, Jochmann K, Lawrence R, Dreier R, Dierker T, Grobe K (2011). Dual roles of the Cardin-Weintraub motif in multimeric Sonic hedgehog. Journal of Biological Chemistry, 286, 23608-23619

Fu H, Qi Y, Tan M, Cai J, Takebayashi H, Nakafuku M, Richardson W, Qiu M (2002). Dual origin of spinal oligodendrocyte progenitors and evidence for the cooperative role of Olig2 and Nkx2.2 in the control of oligodendrocyte differentiation. Development, 129, 681-693

Funderburgh JL (2002). Keratan sulfate biosynthesis. IUBMB Life, 54, 187-194

Guillemot F (2007). Spatial and temporal specification of neural fates by transcription factor codes. Development, 134,3771-3780

Helms AW, Johnson JE (2003). Specification of dorsal spinal cord interneurons. Current Opinion in Neurobiology, 13, 42-49

Hilton BJ, Lang BT, Cregg JM (2012). Keratan sulfate proteoglycans in plasticity and recovery after spinal cord injury. Journal of Neuroscience, 32, 4331-4333

Hirano K, Ohgomori T, Kobayashi K, Tanaka F, Matsumoto T, Natori T, Matsuyama Y, Uchimura K, Sakamoto K, Takeuchi H, Hirakawa A, Suzumura A, Sobue G, Ishiguro N, Imagama S, Kadomatsu K (2013). Ablation of keratan sulfate accelerates early phase pathogenesis of ALS. PloS One, 25, e66969

Imagama S, Sakamoto K, Tauchi R, Shinjo R, Ohgomori T, Ito Z, Zhang H, Nishida Y, Asami N, Takeshita S, Sugiura N, Watanabe H, Yamashita T, Ishiguro N, Matsuyama Y, Kadomatsu K (2011). Keratan sulfate restricts neural plasticity after spinal cord injury. Journal of Neuroscience, 31, 17091-17102

Ito Z, Sakamoto K, Imagama S, Matsuyama Y, Zhang H, Hirano K, Ando K, Yamashita T, Ishiguro N, Kadomatsu K (2010). N-acetylglucosamine 6-O-sulfotransferase-1-deficient mice show better functional recovery after spinal cord injury. Journal of Neuroscience, 30, 5937-5947

Jacob J, Briscoe J (2003). Gli proteins and the control of spinal-cord patterning. EMBO Report, 4, 761-765

Jander S, Schroeter M, Fischer J, Stoll G (2000). Differential regulation of microglial keratan sulfate immunoreactivity by proinflammatory cytokines and colony-stimulating factors. Glia, 30, 401-410

Jones LL, Tuszynski MH (2002). Spinal cord injury elicits expression of keratan sulfate proteoglycans by macrophages, reactive microglia, and oligodendrocyte progenitors. Journal of Neuroscience, 22, 4611-4624

Kadomatsu K, Sakamoto K (2013). Sulfated glycans in network rewiring and plasticity after neuronal injuries. Neuroscience Research

Kuhlbrodt K, Herbarth B, Sock E, Hermans-Borgmeyer I, Wegner M (1998). Sox10, a novel transcriptional modulator in glial cells. Journal of Neuroscience, 18, 237-250

Küspert M, Hammer A, Bösl MR, Wegner M (2011). Olig2 regulates Sox10 expression in oligodendrocyte precursors through an evolutionary conserved distal enhancer. Nucleic Acids Research, 39, 1280-1293

Krylova O, Herreros J, Cleverley KE, Ehler E, Henriquez JP, Hughes SM, Salinas PC (2002). WNT-3, expressed by motoneurons, regulates terminal arborization of neurotrophin-3-responsive spinal sensory neurons. Neuron, 35, 1043-1056

Liu Y, Wu Y, Lee JC, Xue H, Pevny LH, Kaprielian Z, Rao MS (2002). Oligodendrocyte and astrocyte development in rodents: an in situ and immunohistological analysis during embryonic development. Glia, 40, 25-43

Nadanaka S, Ishida M, Ikegami M, Kitagawa H (2008). Chondroitin 4-O-sulfotransferase-1 modulates Wnt-3a signaling through control of E disaccharide expression of chondroitin sulfate. Journal of Biological Chemistry, 283, 27333-27343

Nadanaka S, Kinouchi H, Taniguchi-Morita K, Tamura J, Kitagawa H (2011). Down-regulation of chondroitin 4-O-sulfotransferase-1 by Wnt signaling triggers diffusion of Wnt-3a. Journal of Biological Chemistry, 286, 4199-4208

Ratzka A, Kalus I, Moser M, Dierks T, Mundlos S, Vortkamp A (2008). Redundant function of the heparan sulfate 6-O-endosulfatases Sulf1 and Sulf2 during skeletal development. Developmental Dynamics, 237, 339-353

Ribes V, Balaskas N, Sasai N, Cruz C, Dessaud E, Cayuso J, Tozer S, Yang LL, Novitch B, Marti E, Briscoe J (2010). Distinct Sonic Hedgehog signaling dynamics specify floor plate and ventral neuronal progenitors in the vertebrate neural tube. Genes & Development, 24, 1186-1200

Scardigli R, Schuurmans C, Gradwohl G, Guillemot F (2001). Crossregulation between Neurogenin2 and pathways specifying neuronal identity in the spinal cord. Neuron, 31, 203-217

Shimizu T, Kagawa T, Wada T, Muroyama Y, Takada S, Ikenaka K (2005). Wnt signaling controls the timing of oligodendrocyte development in the spinal cord. Developmental Biology, 282, 397-410

Soula C, Danesin C, Kan P, Grob M, Poncet C, Cochard P (2001). Distinct sites of origin of oligodendrocytes and somatic motoneurons in the chick spinal cord: oligodendrocytes arise from Nkx2.2-expressing progenitors by a Shh-dependent mechanism. Development, 128, 1369-1379

Stolt CC, Rehberg S, Ader M, Lommes P, Riethmacher D, Schachner M, Bartsch U, Wegner M (2002). Terminal differentiation of myelin-forming oligodendrocytes depends on the transcription factor Sox10. Genes & Development, 16, 165-170

Sugimori M, Nagao M, Bertrand N, Parras CM, Guillemot F, Nakafuku M (2007). Combinatorial actions of patterning and HLH transcription factors in the spatiotemporal control of neurogenesis and gliogenesis in the developing spinal cord. Development, 134, 1617-1629

Sun Y, Nadal-Vicens M, Misono S, Lin MZ, Zubiaga A, Hua X, Fan G, Greenberg ME (2001). Neurogenin promotes neurogenesis and inhibits glial differentiation by independent mechanisms. Cell, 104, 365-376

Tanabe Y, Jessell TM (1996). Diversity and pattern in the developing spinal cord. Science, 274, 1115-1123

Touahri Y, Escalas N, Benazeraf B, Cochard P, Danesin C, Soula C (2012). Sulfatase 1 promotes the motor neuron-to-oligodendrocyte fate switch by activating Shh signaling in Olig2 progenitors of the embryonic ventral spinal cord. Journal of Neuroscience, 32, 18018-18034

Uchimura K, Kadomatsu K, El-Fasakhany FM, Singer MS, Izawa M, Kannagi R, Takeda N, Rosen SD, Muramatsu T (2004). N-acetylglucosamine 6-O-sulfotransferase-1 regulates expression of L-selectin ligands and lymphocyte homing. Journal of Biological Chemistry, 279, 35001-35008

Weyers A, Yang B, Solakyildirim K, Yee V, Li L, Zhang F, Linhardt RJ (2013). Isolation of bovine corneal keratan sulfate and its growth factor and morphogen binding. FEBS Journal, 280, 2285-2293

Wojcinski A, Nakato H, Soula C, Glise B (2011). DSulfatase-1 fine-tunes Hedgehog patterning activity through a novel regulatory feedback loop. Developmental Biology, 282, 397-410

Wetts R, Vaughn JE (2000). Manipulation of intracellular calcium has no effect on rate of migration of rat autonomic motor neurons in organotypic slice cultures. Neuroscience, 98, 369-376

Xu X, Cai J, Fu H, Wu R, Qi Y, Modderman G, Liu R, Qiu M (2000). Selective expression of Nkx-2.2 transcription factor in chicken oligodendrocyte progenitors and implications for the embryonic origin of oligodendrocytes. Molecular and Cellular Neuroscience, 16, 740-753

Zhang H, Uchimura K, Kadomatsu K (2006). Brain keratan sulfate and glial scar formation. Annals of the New York Academy of Sciences, 1086, 81-90

Zhou Q, Wang S, Anderson DJ (2000). Identification of a novel family of oligodendrocyte lineage-specific basic helix-loop-helix transcription factors. Neuron, 25, 331-343

Zhou Q, Choi G, Anderson DJ (2001). The bHLH transcription factor Olig2 promotes oligodendrocyte differentiation in collaboration with Nkx2.2. Neuron, 31, 791-807

Zhou Q, Anderson DJ (2002). The bHLH transcription factors OLIG2 and OLIG1 couple neuronal and glial subtype specification. Cell, 109, 61-73

Table1. Primer sequence for RT-PCR

Gene	Accession number	Forward (5'→3')	Reverse (5'→3')
β3GnT7	NM_145222	CCCAACAGCTTCTGGAAGAG	TGGGGTTGACAAAGACATCA
β4GalT4	NM_019804	TGCCAACATCACAGTGGATT	TGCCAGTTCACTCCACACTC
KSGal6ST	NM_023850	CACCAACAGGGTCTTCCGCA	ACCACACCCAGGTCACAAAA
C6ST1	NM_016803	GTTCTTCAACCAGCAGGGCA	CGCCACTTCTCAAACTGCTC
GlcNAc6ST-1	NM_018763	TGAGGTGTTCTTCCTCTATGAGC	CGTACTAGGTGGATGACCTTGAG
GlcNAc6ST-2	NM_011998	GTGTGACATGAGCGTCTTTGAT	GCAGATGATCTTCATGGCATAAT
GlcNAc6ST-3	NM_019950	GAGGAGGTGTGTAAGCCTCTGT	GAAGGCATAGAGTTCACGGATTA
GlcNAc6ST-4	NM_021715	TGCTGCGTGACCCAGGCCTCAA	CATATTGAATGCGAAGGCATC
β-actin	NM_007393	AGGCCAACCGTGAAAAGATGAC	GTACATGGTGGTACCACCAGAC

Figure legends

Figure1. The development of the embryonic spinal cord

The scheme of the developing spinal cord; several secretory factors, such as Wnt, BMP and Shh, act as morphogens. Wnt and BMP are secreted from the roof plate and Shh is secreted from the floor plate and the notochord. They are involved in the patterning of the spinal cord. These domain structures also depend on the transcription factors expression.

Figure2. Keratan sulfate expression in the embryonic spinal cord

(A-C) Cross cryosections of the spinal cord from mouse embryo at embryonic day 10.5 were analyzed for keratan sulfate expression and domain structures by immunohistochemistry. (A) and (D) were stained for Shh (5E1 antibody). (B) and (E) were stained for highly sulfated keratan sulfate (5D4 antibody). (C) and (F) were stained with Nkx2.2 antibody (p3 damin marker). Boxed area in (A), (B) and (C) were shown in (D), (E) and (F) with higher magnification. Highly sulfated keratan sulfate was expressed in the floor plate and the notochord. Scale bar = 200 μm.

Figure3. Expression of keratan sulfate synthesizing enzymes analyzed by RT-PCR

RNA extracted from the embryonic spinal cord at E10.5, E12.5 and E14.5 were subjected to RNA analysis for keratan sulfate synthesizing enzymes. RT-PCR was carried out with the addition of an equal amount of internal control RNA as described in Materials and Methods and separated in a 1.5% agarose gel.

Figure4. The domain structures did not change in the keratan sulfate null mice at E10.5

At E10.5, the embryos were fixed and cross cryosections of the embryonic spinal cord were performed with in situ hybridization, using Math1 (A, B), Olig3 (C, D), Pax7 (E, F), Nkx6.1 (G, H), Olig2 (I, J) and Nkx2.2 (K, L) RNA probes. Right column shows WT results and left column shows keratan sulfate null mouse results. Scale bar = 200 μm.

Figure5. The domain structures seemed to shift ventrally in keratan sulfate null mice at E12.5

At E12.5, embryos were fixed and cross cryosections of the embryonic spinal cord were analyzed by in situ hybridization using Math1 (A, B), Olig3 (C, D), Pax7 (E, F), Nkx6.1 (G, H), Olig2 (I, J) and Nkx2.2 (K, L) RNA probes. Especially, the ventral domain position, Nkx6.1, Olig2 and Nkx2.2, seemed to shift ventrally. Scale bar = 200 μm.

Figure6. Quantification of the ventral shift of the domain structures in keratan sulfate null mice at E12.5

At E12.5, the embryos were fixed and cross cryosections of the embryonic spinal cord were immunostained for Pax7 (Green)/ Pax6 (Red) (Upper column; A, B), Nkx6.1 (Green)/ Olig2 (Red) (middle column; C, D) and Nkx2.2 (Green)/ Olig2 (Red) (Lower column; E, F). Scale bar = 200 μm. (G) Quantification of the percentage of the length of each domain to the length of total spinal cord from roof plate to floor plate. Data are shown as mean ± SEM (N=3).

Figure7. There was no difference in canonical Wnt signaling between WT and keratan sulfate null mice at E10.5 or E12.5

The embryos at E10.5 (A, B) and E12.5 (C, D) were fixed and cross cryosections of the embryonic spinal cord were analyzed using in situ hybridization using Axin2 RNA probe. Axin2 is a canonical Wnt signaling reporter. Scale bar = 200 μm.

Figure8. Pattern of Shh signaling differed between WT and keratan sulfate null mice at E12.5

The embryos at E10.5 (A, B), E11.5 (C, D) and E12.5 (E, F) were fixed and cross

cryosections of the embryonic spinal cord were analyzed by in situ hybridization using Patched1 RNA probe. Patched1 is a Shh signaling reporter. The black parenthese indicated the pMN domain. Scale bar = 200 μm.

Figure9. The change of Sulf1 expression pattern from E10.5 to E12.5

The embryos at E10.5 (A, B), E11.5 (C, D) and E12.5 (E, F) were fixed. Cross cryosections of the embryonic spinal cord were analyzed by in situ hybridization using Sulf1 RNA probe and immunohistochemistry using Olig2 antibody. Sulf1 is heparan sulfate endosulfatase. The black parenthese indicated the pMN domain. Sulf1 eapression was expanded dorsally. Scale bar = 200 μm.

Figure10. The dorsal expansion of Sulf1 expression was decreased in the E12.5 keratan sulfate null mice

Embryos at E12.5 (A, B) were fixed. Cross cryosections of the embryonic spinal cord were analyzed by in situ hybridization using Patched1 and Sulf1 RNA probes and immunohistochemistry using Olig2 antibody. (A) Comparison between Patched1 and Sulf1 expression. (B) Quantification of the percentage of the length of Sulf1 expression to the length of total spinal cord from roof plate to floor plate. Data are shown as mean ± SEM (WT; N=4, KS-null; N=3). Scale bar = 100 μm.

Figure11. The number of oligodendrocyte precursor cells was remarkably decreased in keratan sulfate null mice at E12.5 and E14.5

Embryos at E12.5 (A, B) and E14.5 (D, E) were fixed. Cross cryosections of the embryonic spinal cord were analyzed by in situ hybridization using PDGFRα RNA probe. PDGFRα is a marker for oligodendrocyte precursor cells. Scale bar = 200 μm. (A, B) PDGFRα positive cells were expressed from the pMN domain and expanded around the pMN domain. (C) Quantification of the number of PDGFRα positive cells. Data are shown as mean ± SEM (WT; N=4, KS-null; N=4). (F) Quantification of the number of PDGFRα positive cells. Data are shown as mean ± SEM (WT; N=5, KS-null; N=5). PDGFRα; Platelet-derived growth factor receptor alpha.

Figure12. The reduction of oligodendrocyte was recoverd in keratan sulfate null mice until P0

After birth, cross cryosections of the postnatal spinal cord were immunostained for MBP and Olig2. MBP and Olig2 is a marker for mature oligodendrocyte. P0 spinal cord sections of WT (A) and keratan sulfate null (B) embryos stained with MBP antibody. At P0, Olig2 positive cells populate the entire spinal cord and are present in similar densities in WT (C) and keratan sulfate null (D) embryos. Scale bar = 200 μm.

Figure13. The generation of motor neurons was continued in keratan sulfate null

mice until at E12.5

Embryos at E12.5 (A, B, D and E) were fixed. Cross cryosections of the embryonic spinal cord were immunostained for Islet1/2. Islet1/2 is a marker for motor neurons. (A, B) Mature motor neurons in ventral horn has two types, AMNs and SMNs. (C) Quantification of the number of Islet1/2 positive cells Data are shown as mean ± SEM (WT; N=4, KS-null; N=4). (D, E) Immature motor neurons were migrated from pMN domain. Scale bar = 200 μm. AMNs; Autonomic motor neuros, SMNs; Somatic motor neurons.

Figure14. Increased apoptosis and microglia activation in the ventral horn of keratan sulfate null mice at E14.5

Embryos at E14.5 (A, B, D and E) were fixed. Cross cryosections of the embryonic spinal cord were immunostained for Cleaved Caspase-3 and Iba1 antibody. Cleaved Caspase-3 is a marker for apoptosis (A, B). Iba1 is a marker for microglia (D, E). (C) Quantification of the number of Cleaved Caspase-3 positive cells Data are shown as mean ± SEM (WT; N=7, KS-null; N=6). When the microglia activated, the morphology formed amoeboid shape. Scale bar = 100 μm.

Figure15. Switching of ologodendocyte generation was delayed in the keratan sulfate null mice at E12.5

(A) The scheme of switching of oligodendrocyte generation in the embryonic spinal cord; Oligodendroglial specification is marked by the induction of the Sox10 expression. Following that, coexpression of Olig2 with Nkx2.2 promotes oligodendrocyte differentiation. The embryos at E12.5 were fixed. Cross cryosections of the embryonic spinal cord were analyzed by in situ hybridization using Sox10 RNA probe (B and C) and immunohistochemistry using Olig2 and Nkx2.2 antibody (D and E). (D and E) Cross cryosections were double-immunostained for Olig2 and Nkx2.2. Green color was Nkx2.2, red color was Olig2, white color is Olig2 and Nkx2.2 double positive cells (white arrow). (F) Quantification of the ratio of Olig2+; Nkx2.2+ to Olig2+ cells. Data are shown as mean ± SEM (WT; N=6, KS-null; N=5). Scale bar = 100 μm.

Figure16. Specification of motor neuron was enhanced in the keratan sulfate null mice at E12.5

(A) The scheme of specification of motor neuron in the embryonic spinal cord; The basic helix-loop-helix (bHLH)-class transcription factors Ngn1/2 and Olig1/2 play important roles on motor neuron generation. Coexpression of Olig2 and Ngn2 in pMN domain occurs during the period of motor neuron generation, however, at later stages when oligodendrocytes were produced, Ngn2 expression becomes downregulated. (B-F) The embryos at E12.5 were fixed. Cross cryosections of the embryonic spinal cord were analyzed by in situ hybridization and immunohistochemistry, using Ngn2 RNA probe

and Olig2 antibody (B-E). White boxed area in (D) and (E) were shown in (B) and (C) with higher magnification. Black arrows showed Ngn2 and Olig2 double positive cells. (F) Quantification of the ratio of Olig2+; Ngn.2+ to Olig2+ cells. Data are shown as mean ± SEM (WT; N=3, KS-null; N=3). Scale bar = 200 μm (B and C), 100μm (D and E).

Figure17. Shh distribution and regulation by acidic sugar chains in the keratan sulfate null mice

The scheme of Shh distribution and regulation by acidic sugar chains in the embryonic spinal cord before oligodendrocyte development; Highly sulfated localize in the floor plate and bind to Shh. Sulf1 is expressed in the floor plate and expanded dorsally. 6O-sulfated heparan sulfate has a capacity of binding to Shh, but 6O-non-sulfated heparan sulfate was weak to bind to Shh. Then highly sulfated keratan sulfate and 6O-sulfated-heparan sulfate transports Shh protein out of Sulf1 expression region. When Shh signaling accumulates in the pMN domain, oligodendrocyte development begins from E12.5.

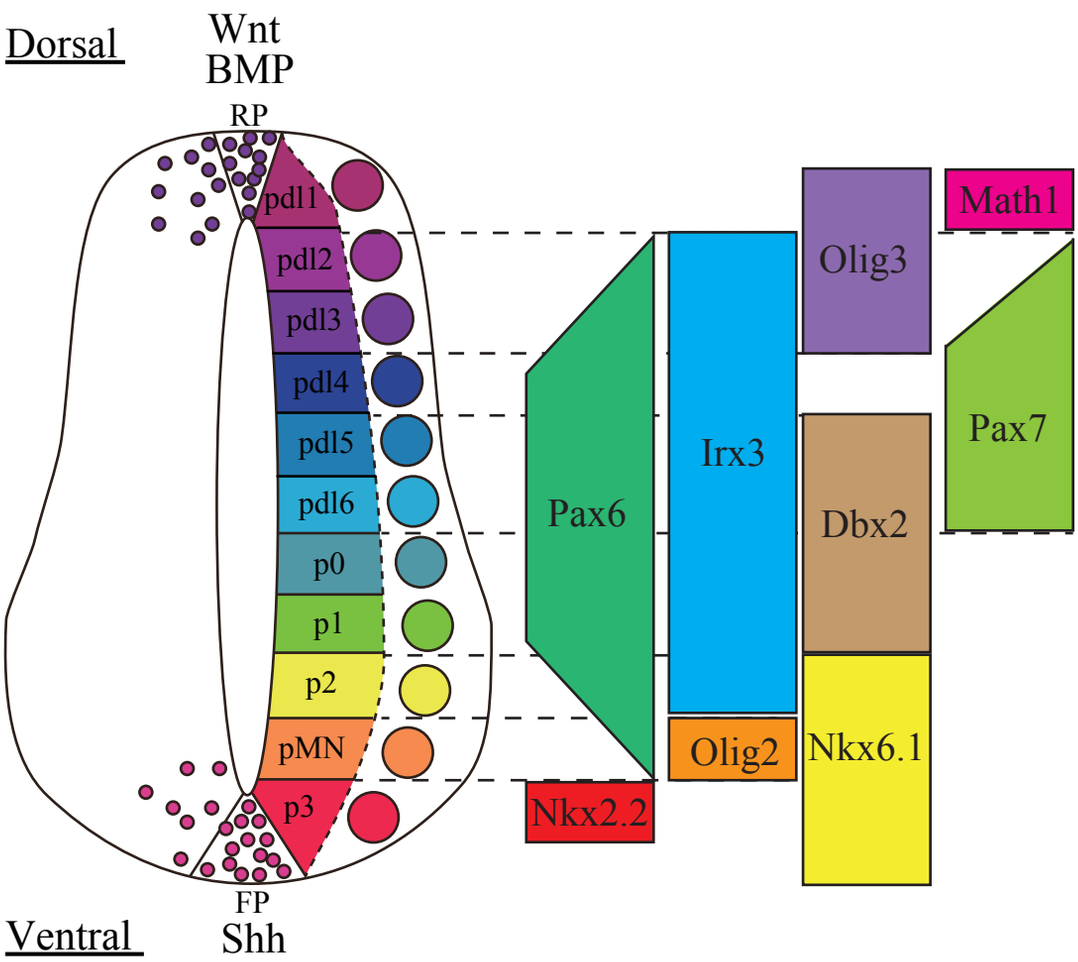
Dorsal
Wnt
BMP
RP
pdl1
pdl2
pdl3
pdl4
pdl5
pdl6
p0
p1
p2
pMN
p3
FP
Ventral
Shh
Pax6
Irx3
Olig3
Math1
Pax7
Dbx2
Olig2
Nkx6.1
Nkx2.2

Figure1

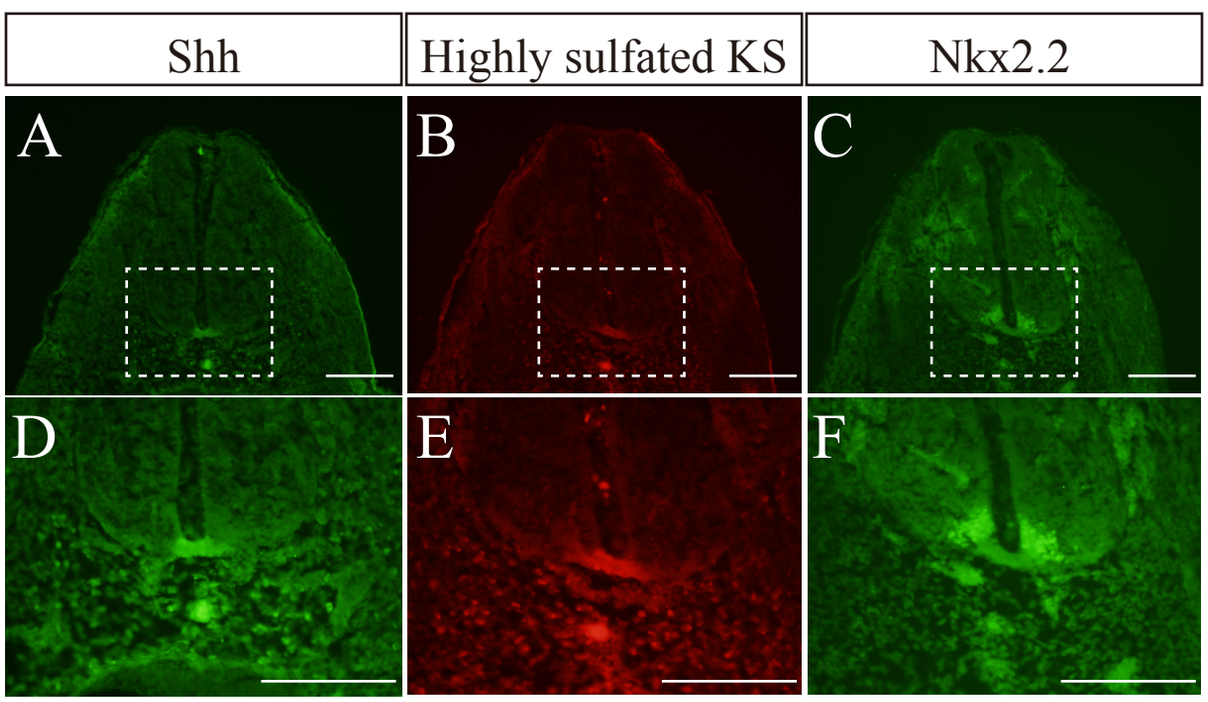

Figure2

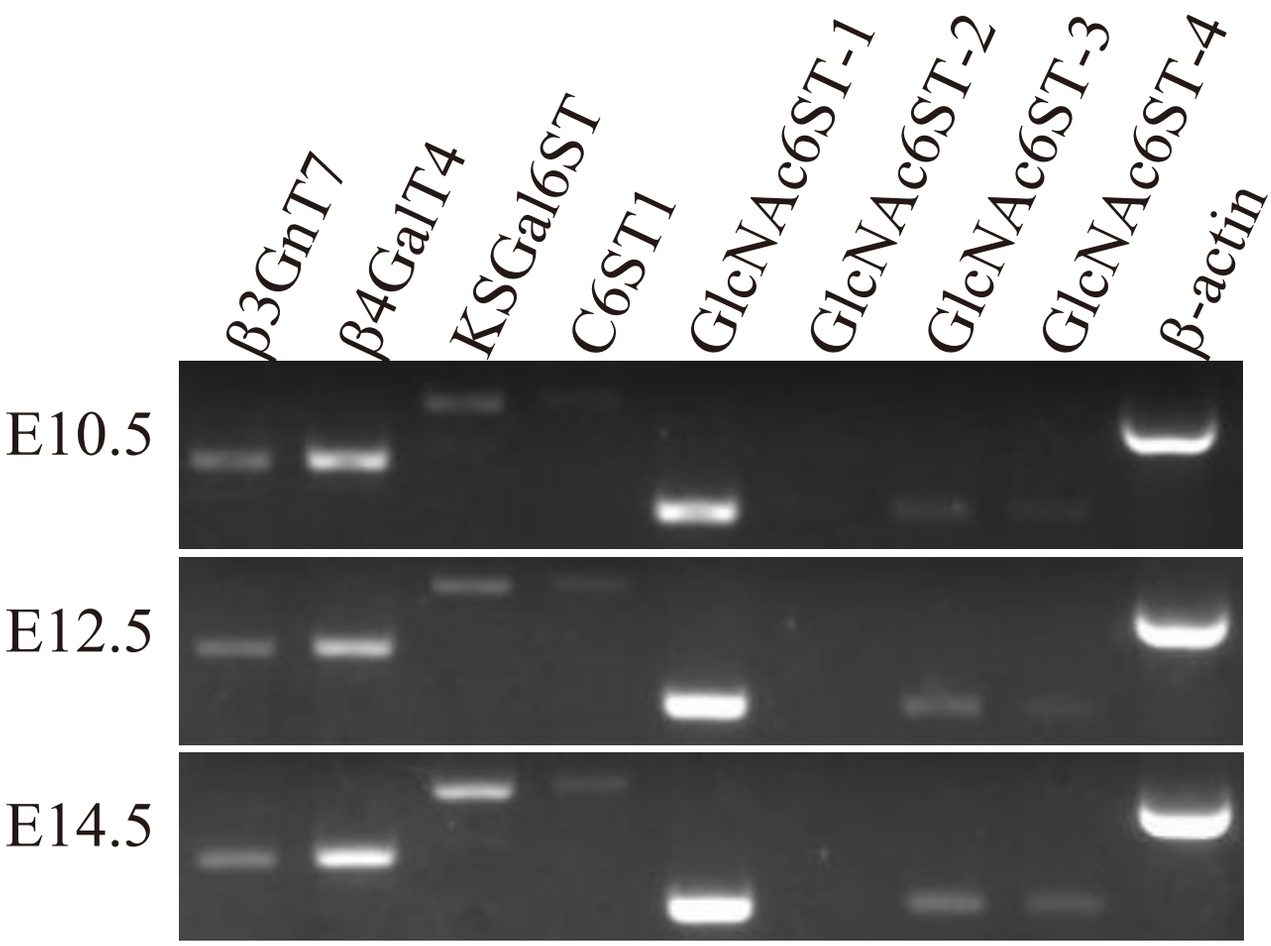
β3GnT7
β4GalT4
KSGal6ST
C6ST1
GlcNAc6ST-1
GlcNAc6ST-2
GlcNAc6ST-3
GlcNAc6ST-4
β-actin
E10.5
E12.5
E14.5

Figure3.

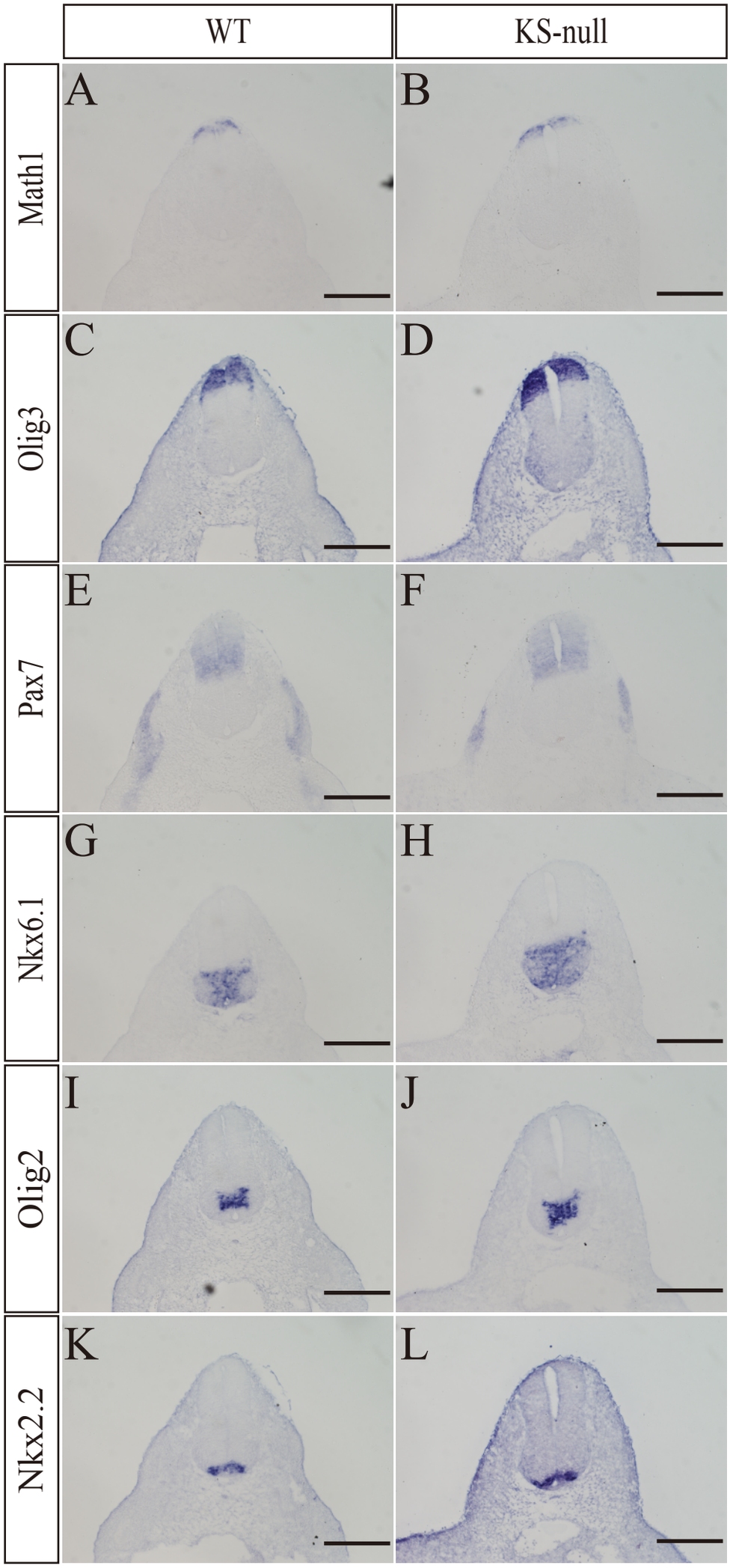

Figure4

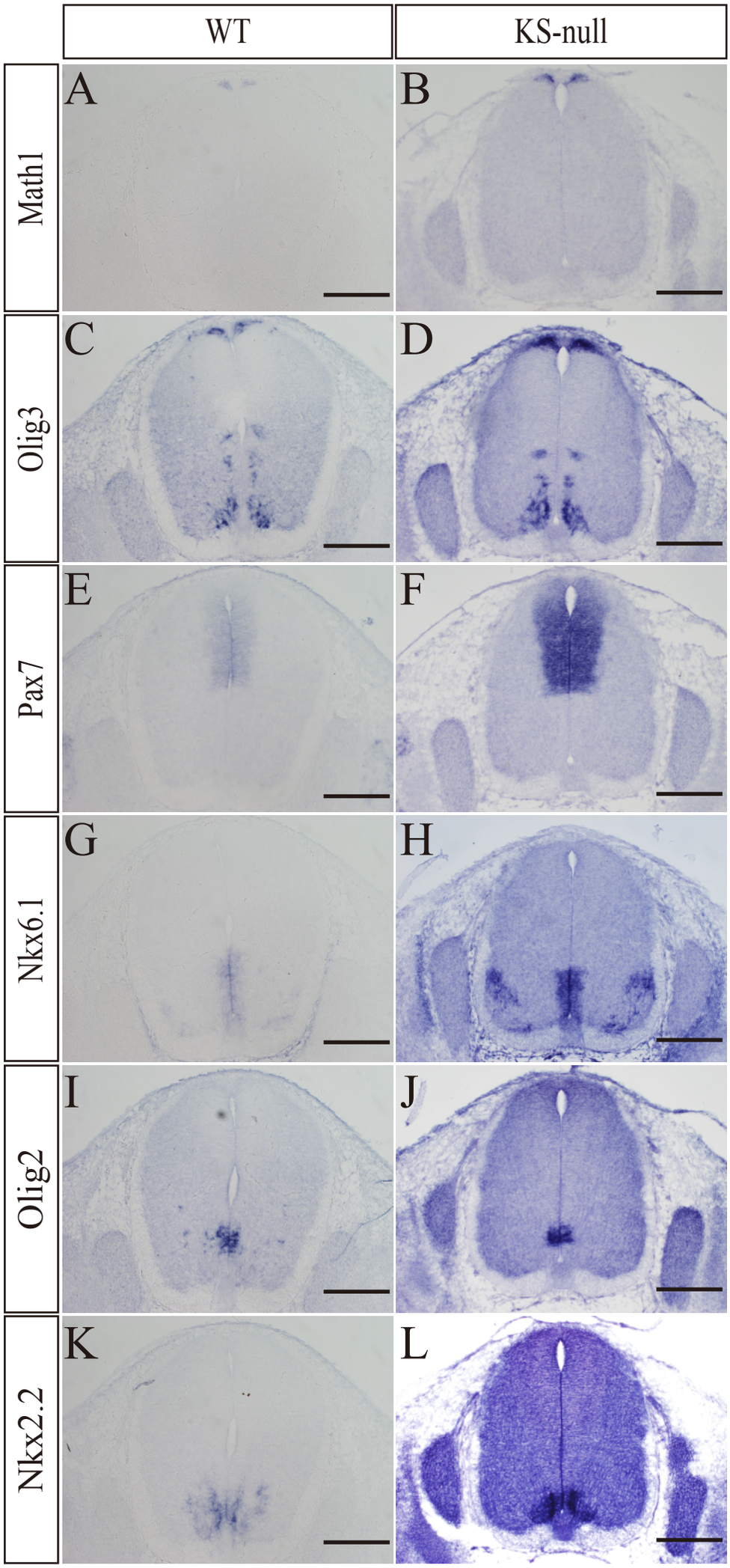

Figure5

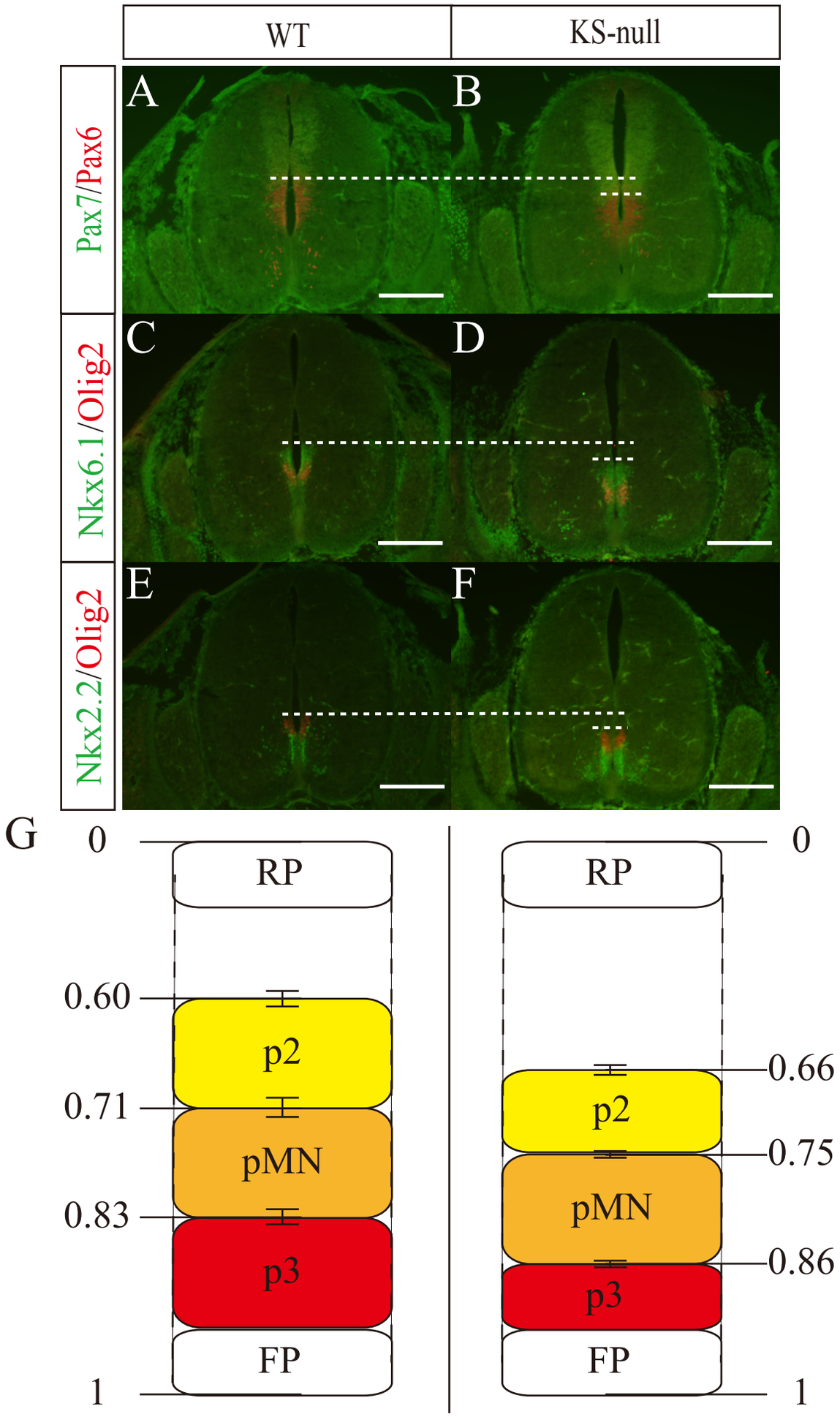
WT
KS-null
Pax7/Pax6
Nkx6.1/Olig2
Nkx2.2/Olig2
A
B
C
D
E
F
G
0
RP
0.60
p2
0.71
pMN
0.83
p3
1
FP
0
RP
0.66
p2
0.75
pMN
0.86
p3
FP
1

Figure6

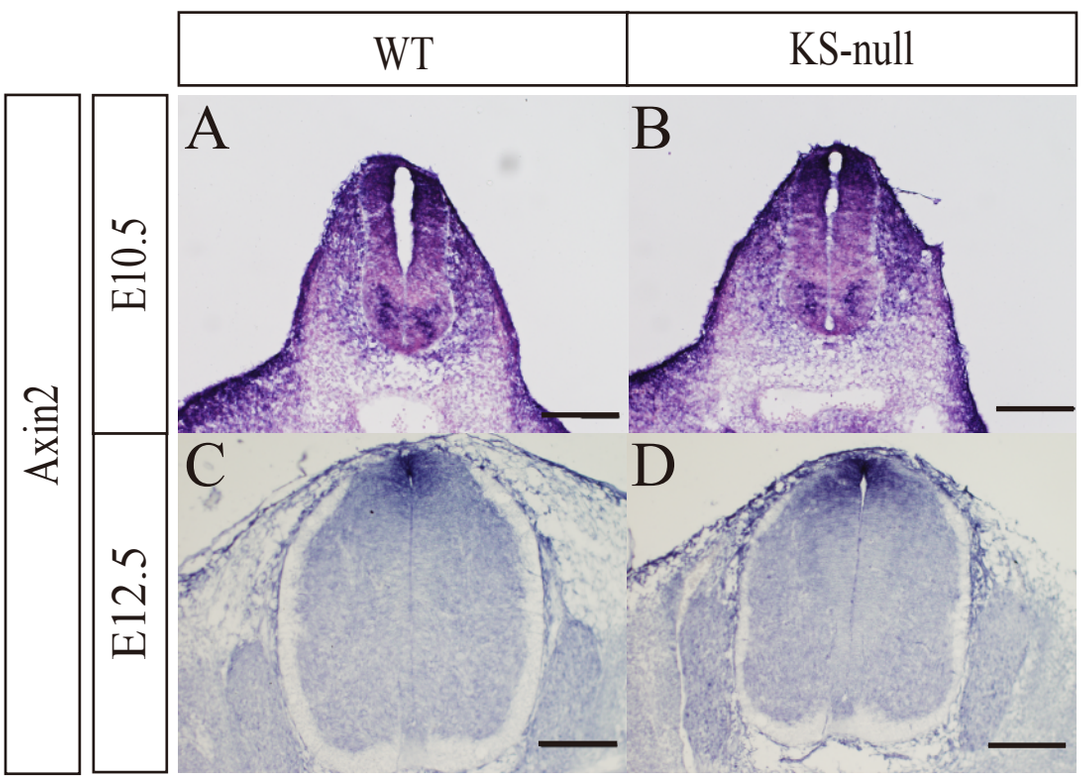

Figure7

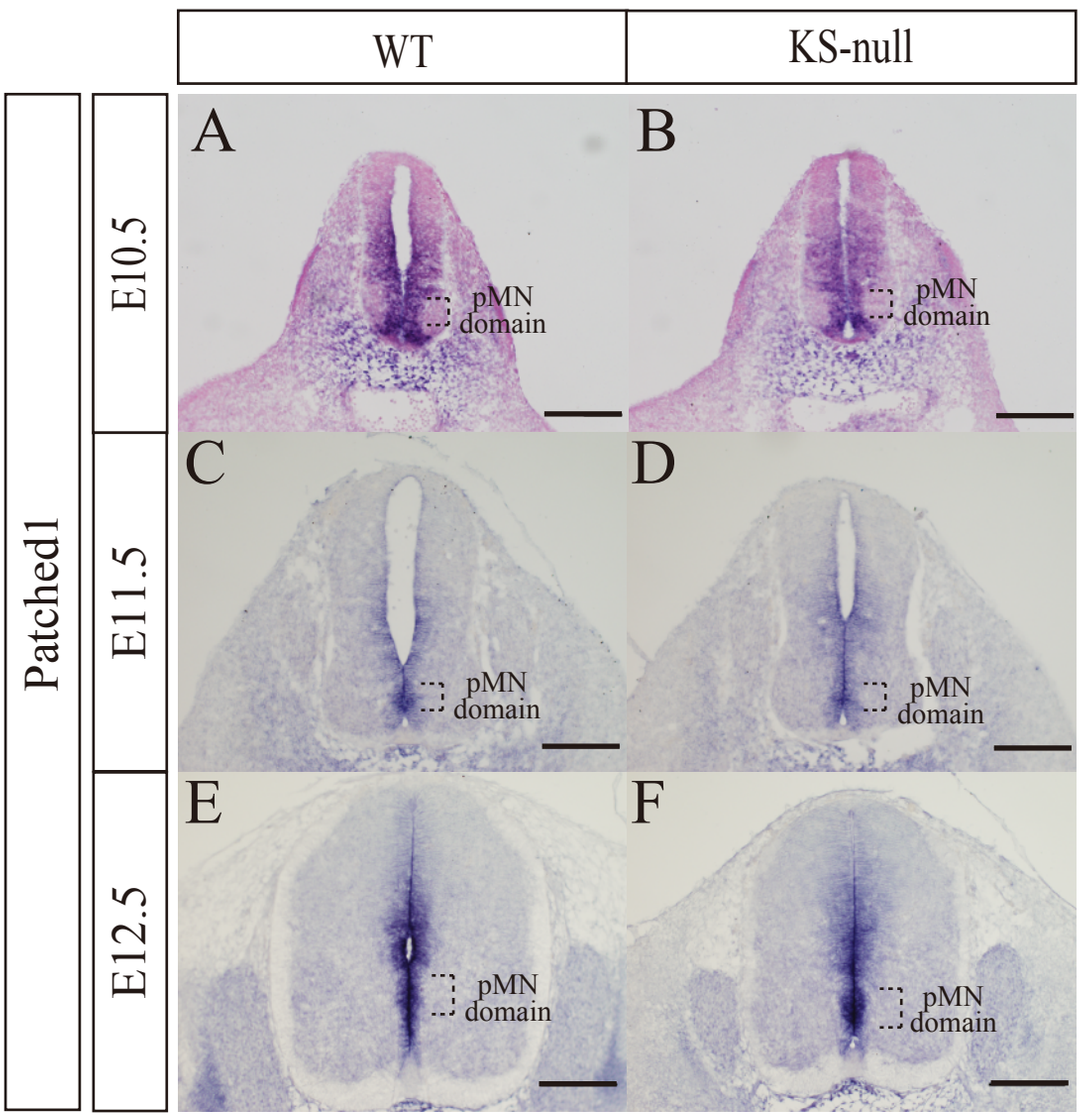

Figure8

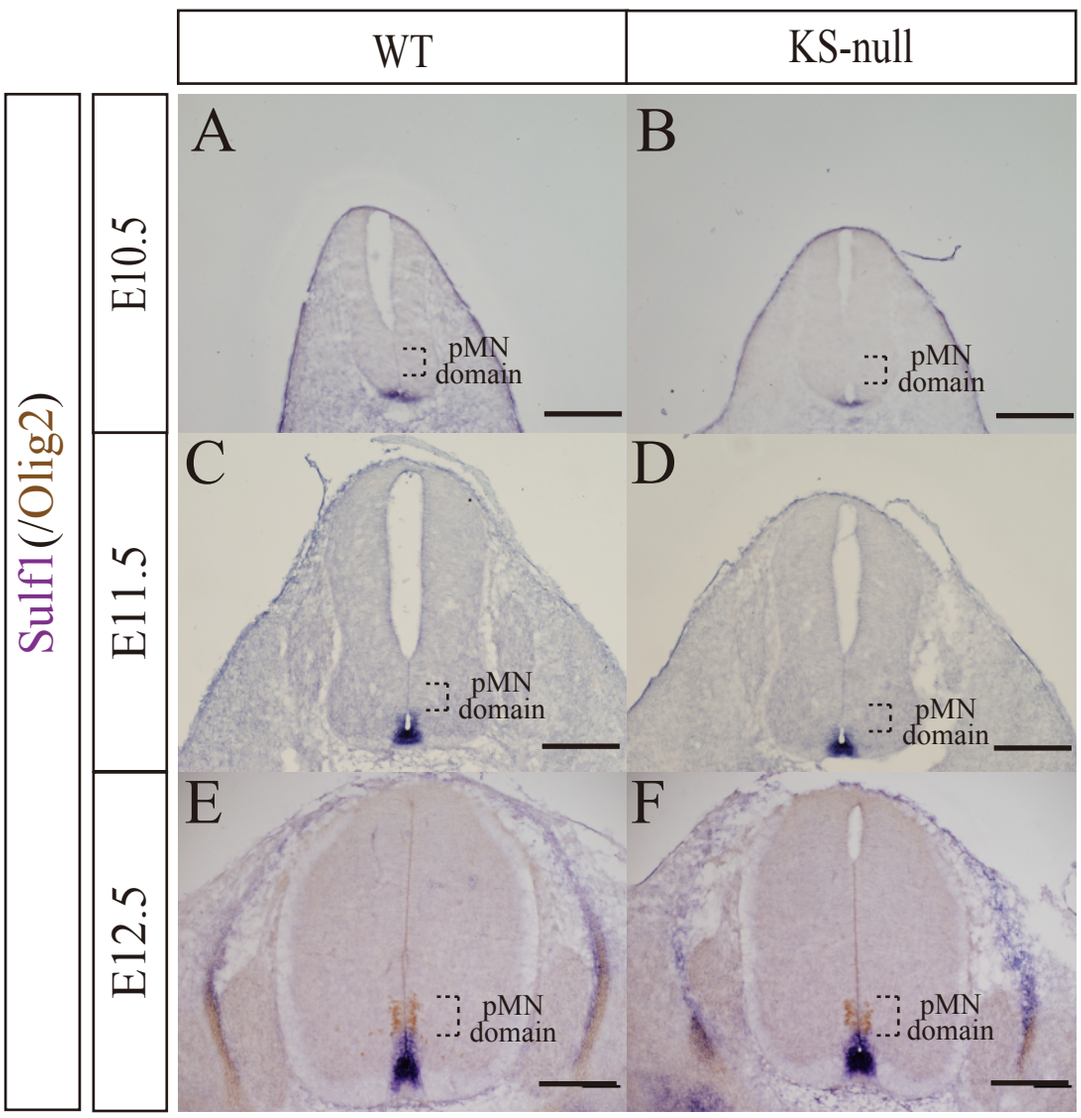

Figure9

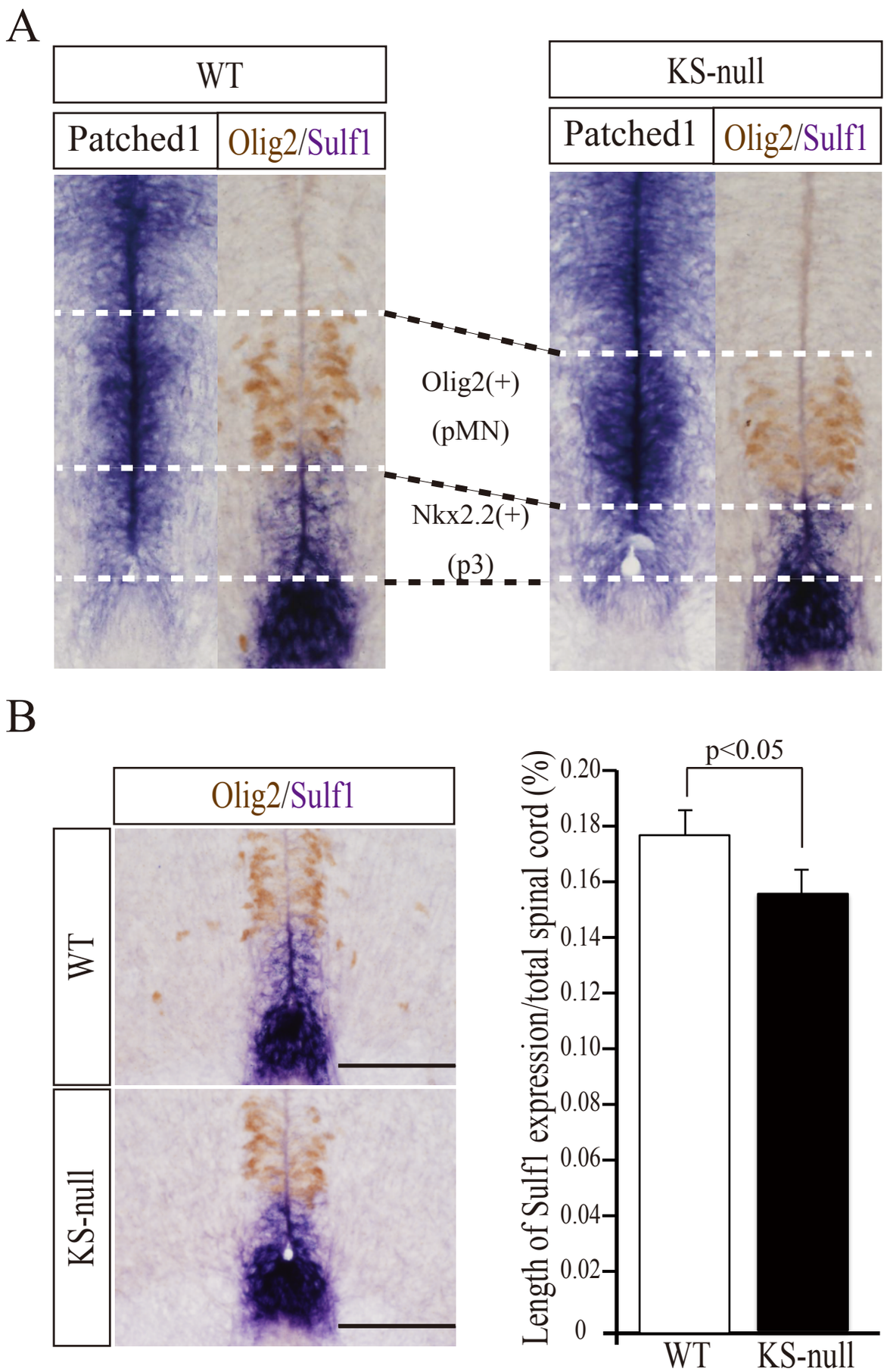
A
WT
Patched1
Olig2/Sulf1
KS-null
Patched1
Olig2/Sulf1
Olig2(+)
(pMN)
Nkx2.2(+)
(p3)
B
Olig2/Sulf1
WT
KS-null
p<0.05
Length of Sulf1 expression/total spinal cord (%)
0.20
0.18
0.16
0.14
0.12
0.10
0.08
0.06
0.04
0.02
0
WT
KS-null

Figure10

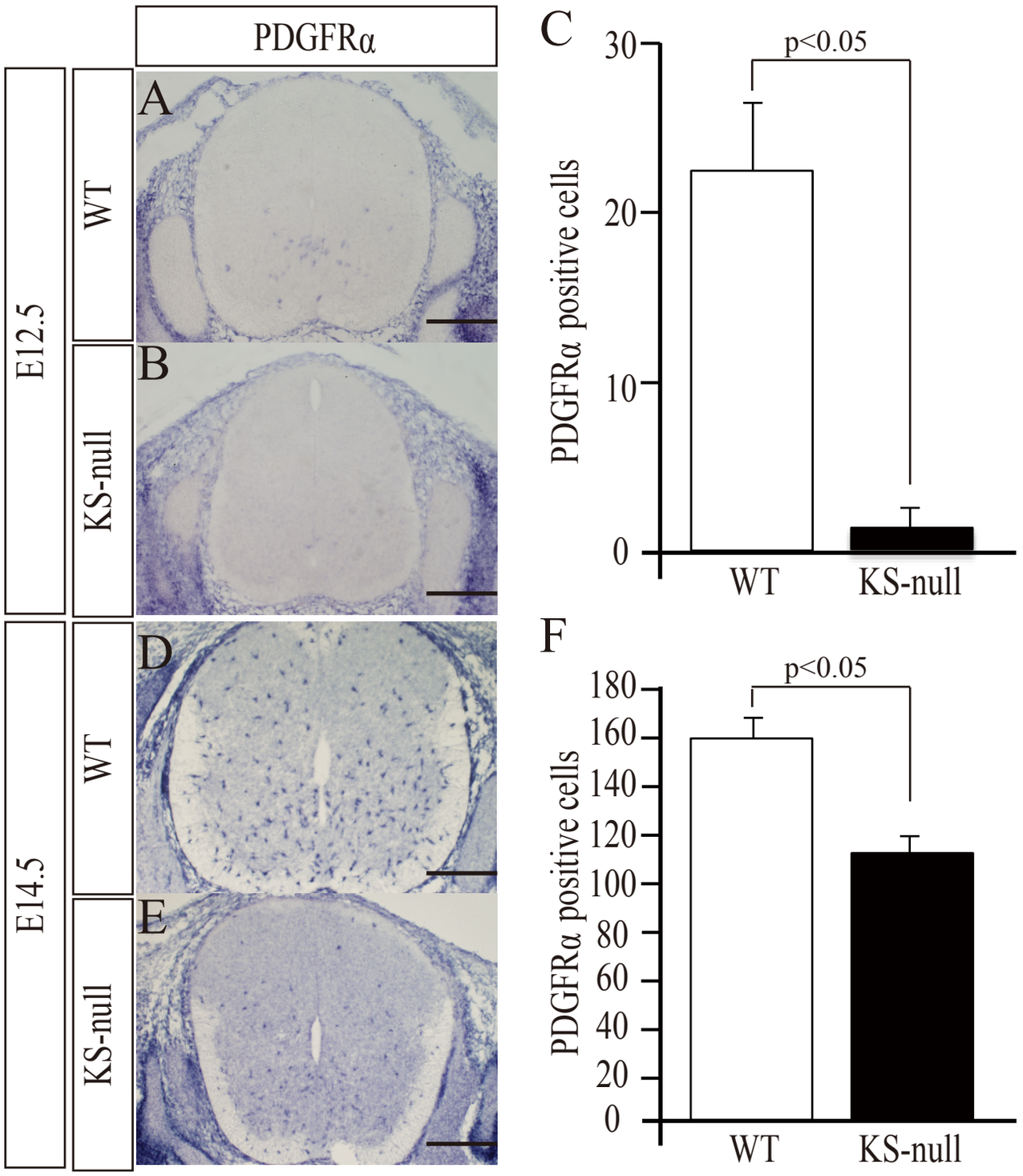
PDGFRα
E12.5
WT
KS-null
E14.5
WT
KS-null
A
B
D
E
C
PDGFRα positive cells
p<0.05
30
20
10
0
WT
KS-null
F
PDGFRα positive cells
p<0.05
180
160
140
120
100
80
60
40
20
0
WT
KS-null

Figure11

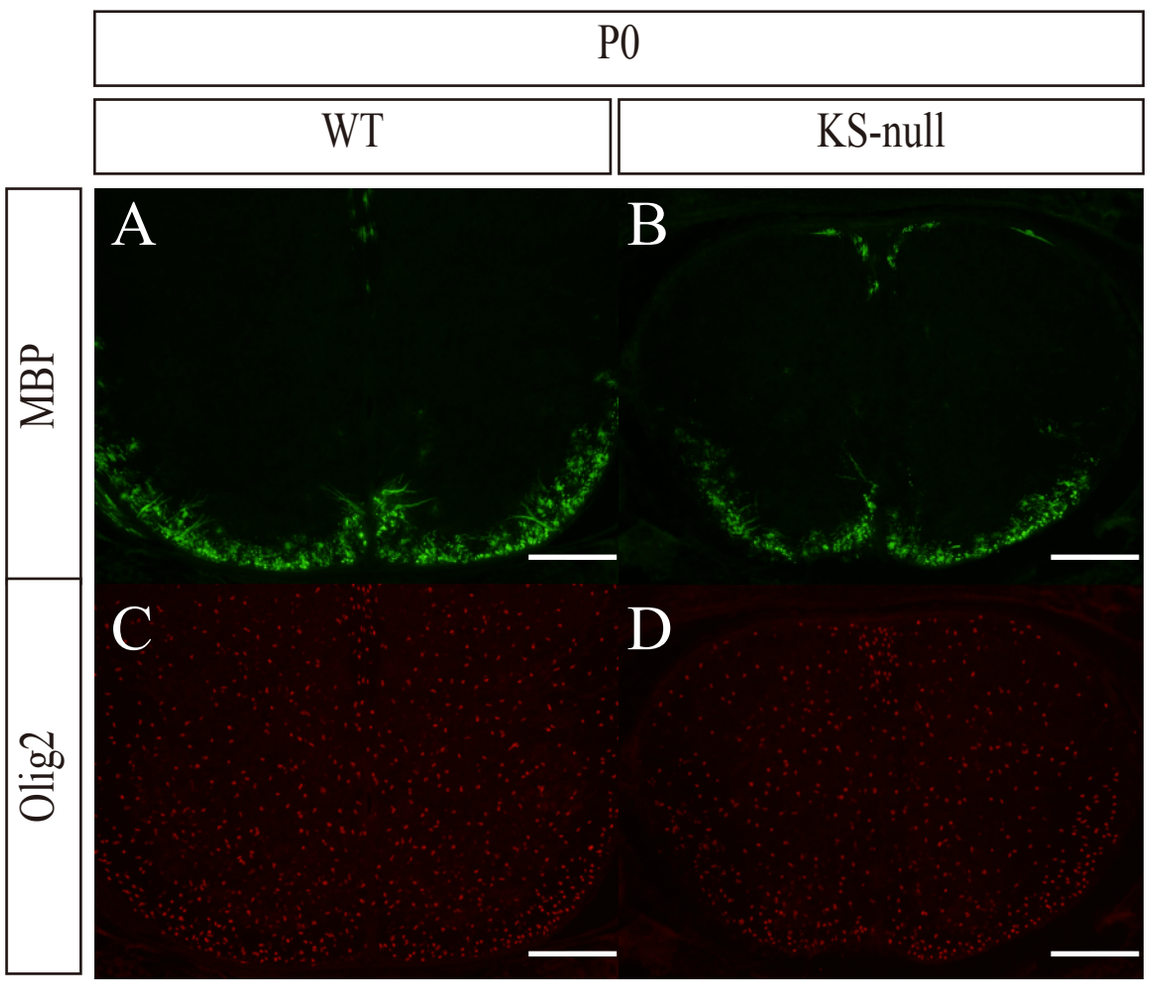

Figure12

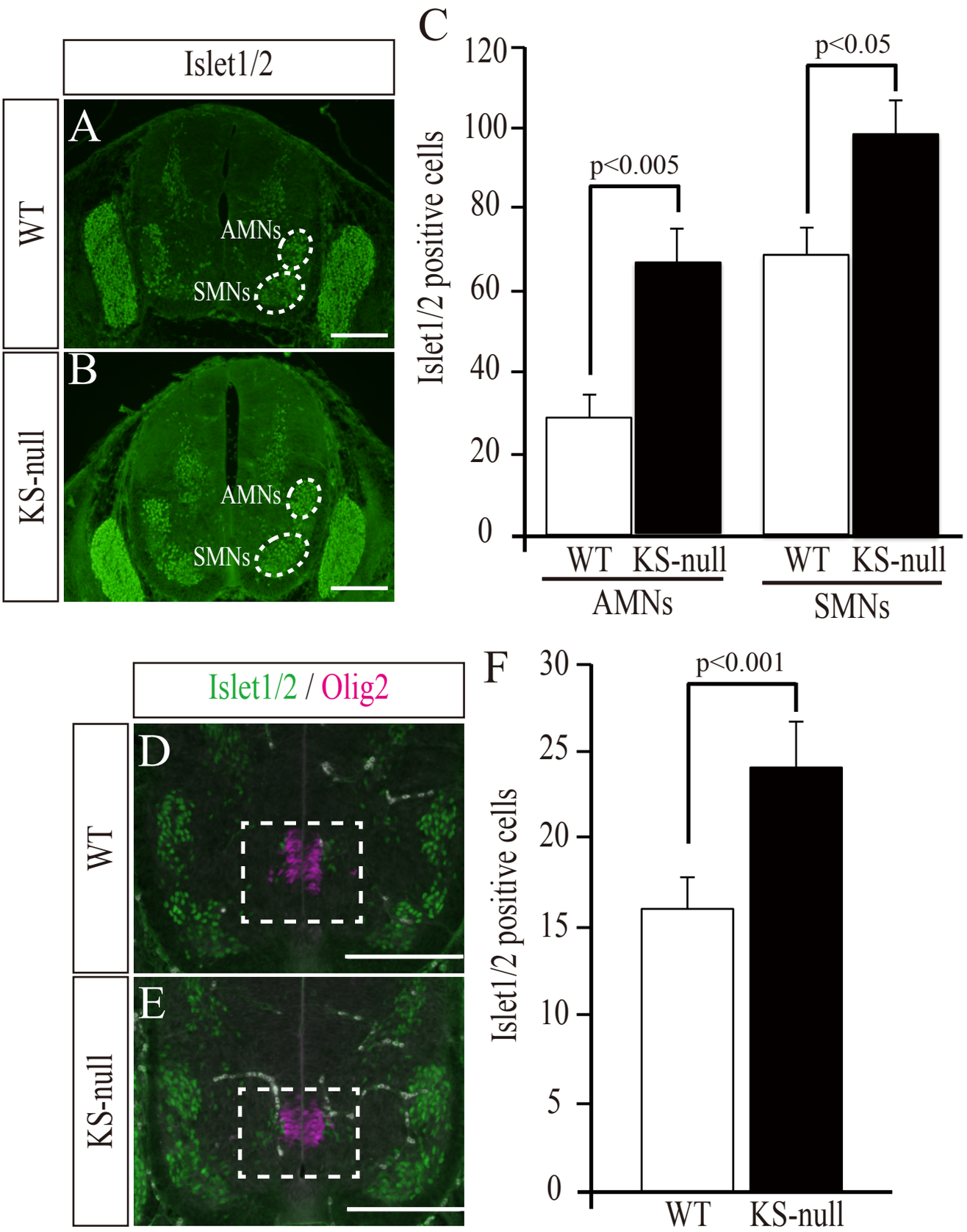
Islet1/2
WT
KS-null
A
B
AMNs
SMNs
AMNs
SMNs
C
Islet1/2 positive cells
120
100
80
60
40
20
0
p<0.005
p<0.05
WT
KS-null
WT
KS-null
AMNs
SMNs
Islet1/2 / Olig2
WT
KS-null
D
E
F
Islet1/2 positive cells
30
25
20
15
10
5
0
p<0.001
WT
KS-null

Figure13

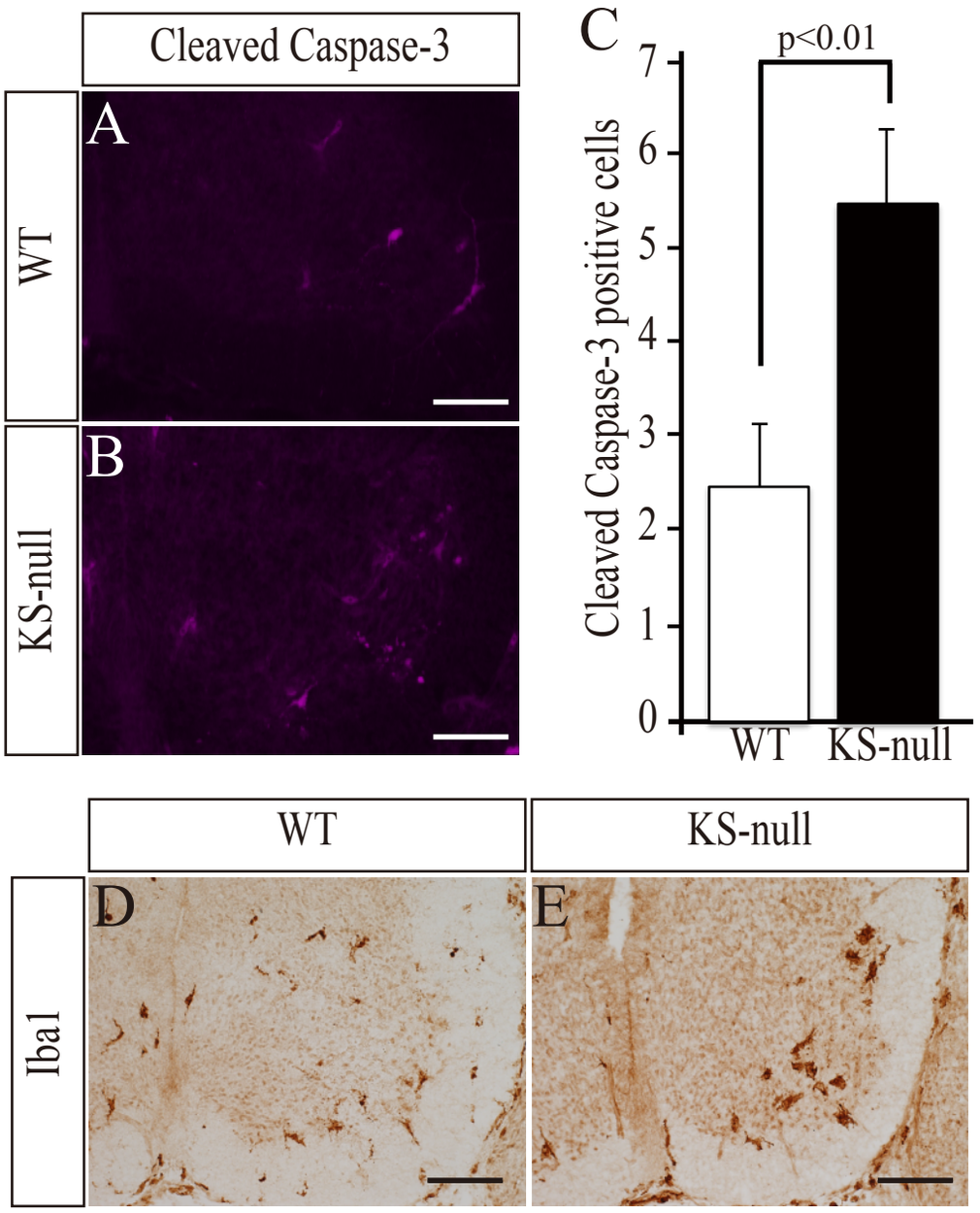
Cleaved Caspase-3
A
WT
B
KS-null
C
p<0.01
Cleaved Caspase-3 positive cells
0
1
2
3
4
5
6
7
WT
KS-null
WT
KS-null
D
E
Iba1

Figure14

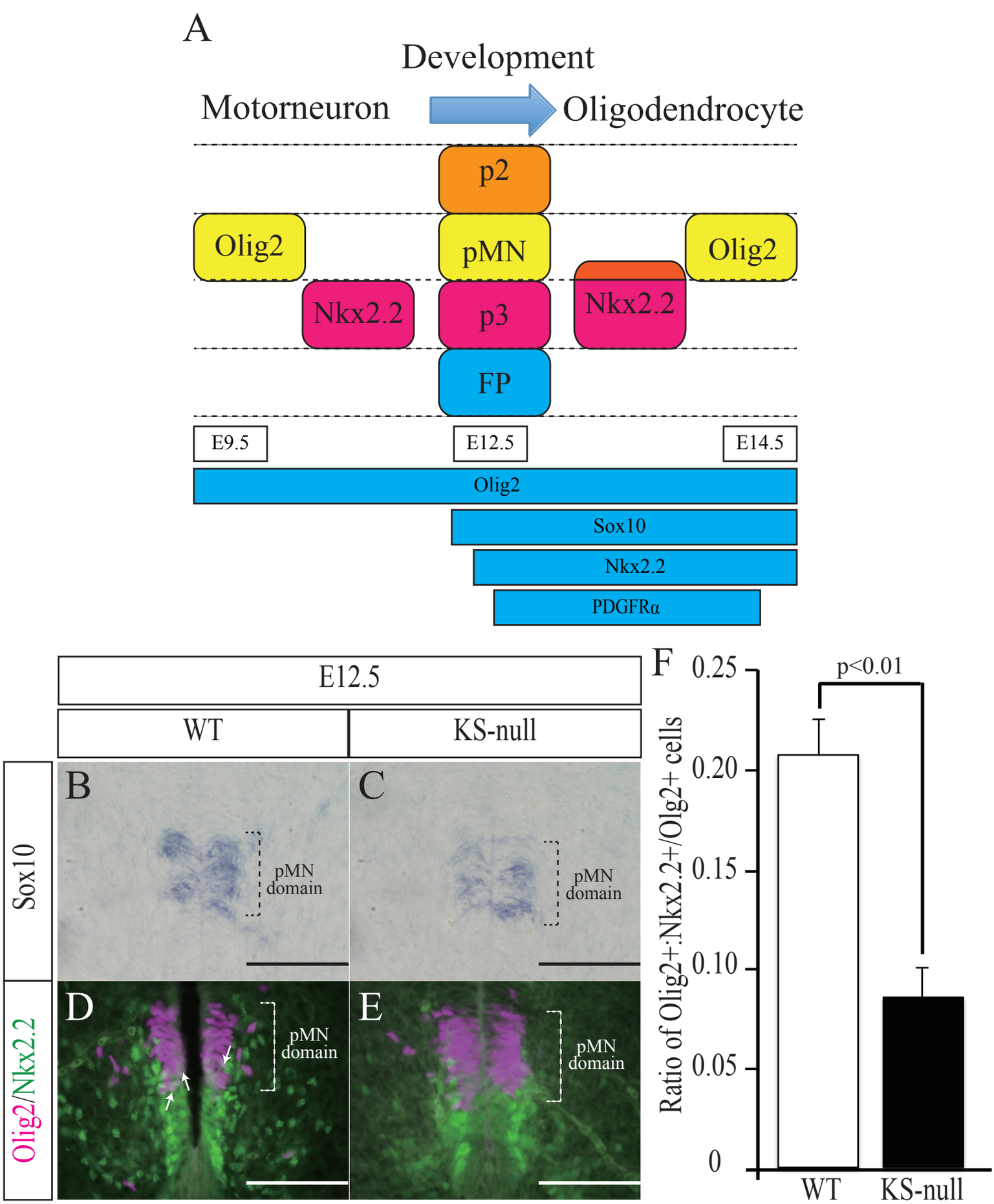
A
Development
Motorneuron
Oligodendrocyte
p2
Olig2
pMN
Olig2
Nkx2.2
p3
Nkx2.2
FP
E9.5
E12.5
E14.5
Olig2
Sox10
Nkx2.2
PDGFRα
E12.5
WT
KS-null
Sox10
Olig2/Nkx2.2
B
C
D
E
pMN domain
F
p<0.01
Ratio of Olig2+:Nkx2.2+/Olig2+ cells
0.25
0.20
0.15
0.10
0.05
0
WT
KS-null

Figure15

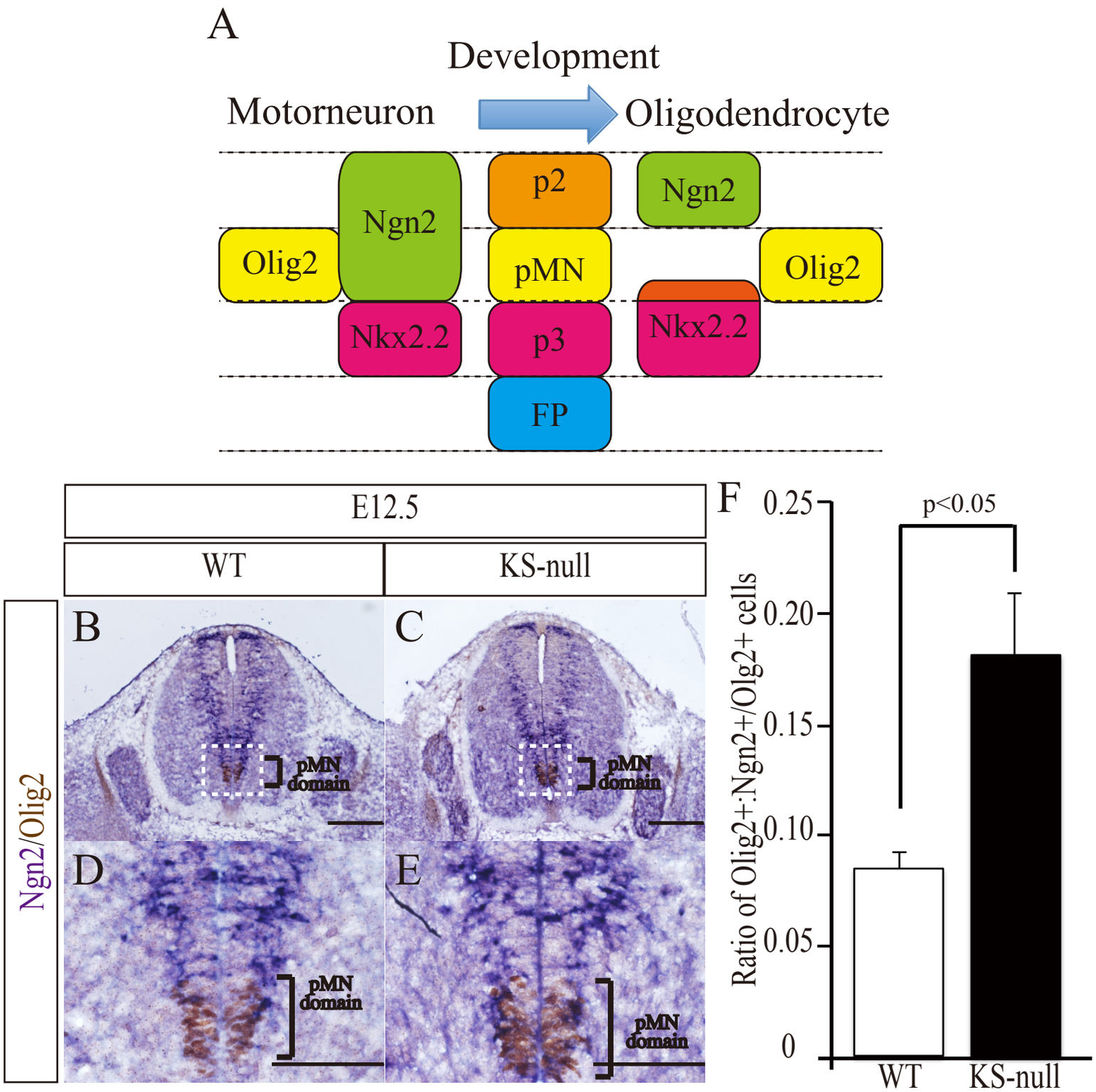
A
Development
Motorneuron
Oligodendrocyte
Olig2
Ngn2
Nkx2.2
p2
pMN
p3
FP
Ngn2
Olig2
Nkx2.2
E12.5
WT
KS-null
Ngn2/Olig2
B
C
D
E
pMN domain
F
p<0.05
Ratio of Olig2+:Ngn2+/Olig2+ cells
0.25
0.20
0.15
0.10
0.05
0
WT
KS-null

Figure16

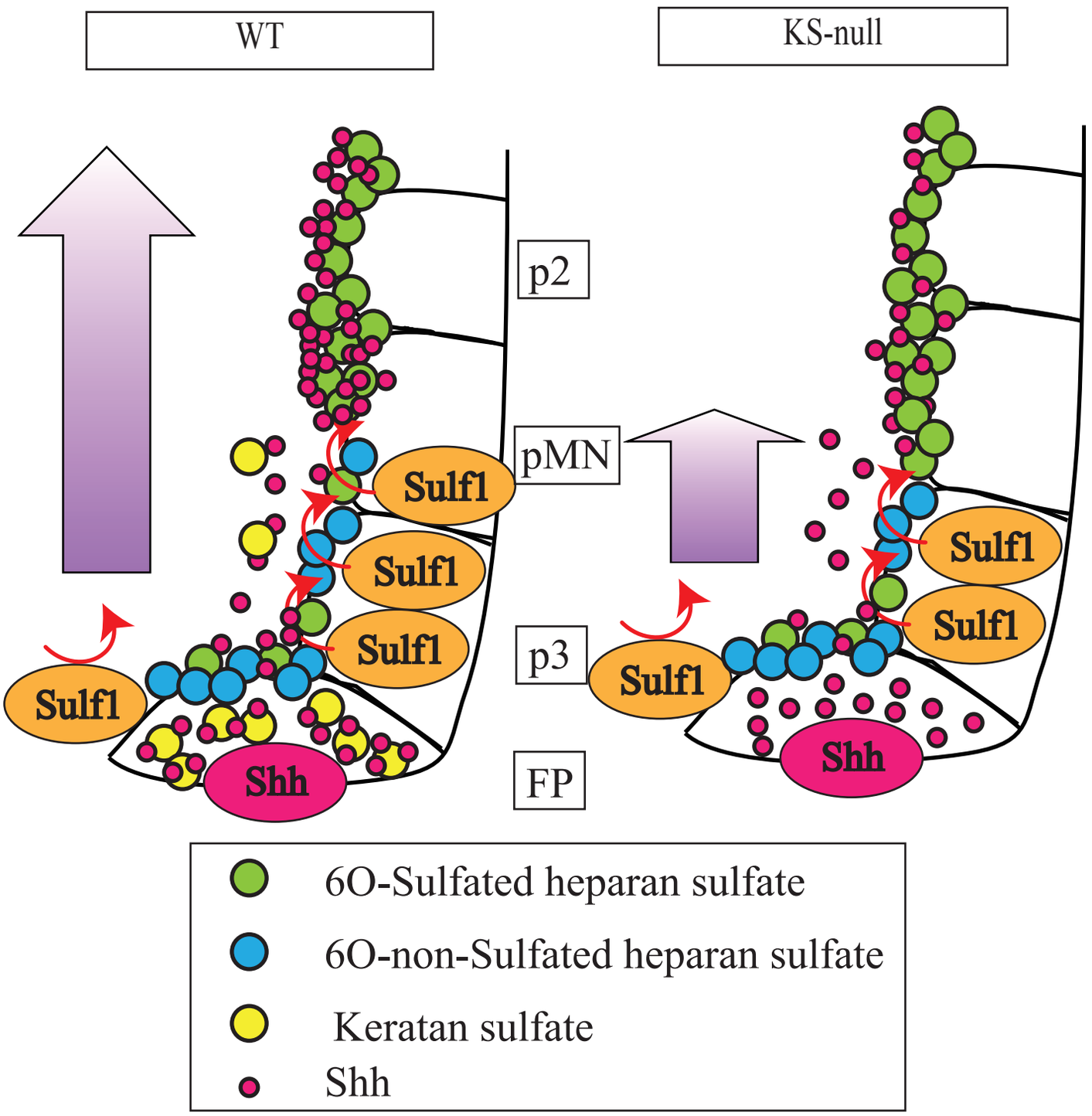
WT
KS-null
p2
pMN
p3
FP
Sulf1
Sulf1
Sulf1
Sulf1
Sulf1
Sulf1
Shh
Shh
6O-Sulfated heparan sulfate
6O-non-Sulfated heparan sulfate
Keratan sulfate
Shh

Figure17